Modeling foot-and-mouth disease dissemination in Brazil and evaluating the effectiveness of control measures

Nicolas C. Cardenas[1], Francisco P. N. Lopes[2], Gustavo Machado[1,*]

[1] Department of Population Health and Pathobiology, College of Veterinary Medicine, North Carolina State University, Raleigh, NC, USA

[2] Departamento de Defesa Agropecuária, Secretaria da Agricultura, Pecuária e Desenvolvimento Rural, Porto Alegre, Brazil

Abstract

Foot-and-mouth disease (FMD) infects multiple food-animal species and thus is capable of disseminating among ungulate species with distinct transmission rates. Here, we present a multilevel compartmental stochastic model, that takes into account population dynamics, births, and deaths, and explicit representation of species-specific transmission dynamics. The model considered two major modes of transmission, within-farm and between-farm Susceptible-Exposed-Infected-Recovered (SEIR) transmission with species-specific transmission dynamics. Our model outcomes are the number of secondarily infected animals and farms, spatial dissemination distances, the role of major transmission pathways, and the effectiveness of different scenarios to control outbreaks. We demonstrated that after 20 days of FMD dissemination, the median number of infected farms when considered all species was 8 (IQR: 3-22), and 7 (IQR: 3-22) when considered only bovine, 3 (IQR: 1-6) for swine farms, and 1 (IQR: 1-1) for small ruminants. We demonstrated that animal movement was the primary route for dissemination in the first days of epidemics, while at ten days, spatial transmission was the predominant cause of bovine infections and between-farm animal movements led to the most

swine infections. Furthermore, we have also shown that the median distance between seeded and secondary infections was 5.77 km (IQR: 1-10.29 km), with some long-range dissemination at 695.40 km. The depopulating of 12 and vaccinating of 15,000 farms per day after 20 days of FMD silent dissemination, faded 93.4% of the epidemics with a median of 9 (IQR: 3-23, max: 221) infected farms within 54 days of the deployment of control actions. In conclusion, the developed transmission model allows for cross-species transmission to be considered in FMD policymaking, and the software implementation facilitates the adaption of scientific-based support to FMD planning.

Keywords: dynamical models, infectious disease control, epidemiology, transmission, targeted control.

1. Introduction

Foot-and-mouth disease (FMD) is an infectious disease in cloven-hoofed animals that affects multiple species, including pigs, sheep, goats, and wildlife (Davies, 2002; Paton et al., 2018). During the 2001 FMD epidemic in the U.K. and The Netherlands, more than 6.7 million animals were slaughtered, including healthy (preemptively) and infected farms (Bouma et al., 2003; Thompson et al., 2002). The majority of infected animals in both outbreaks were not unique to one species; for example, infection was detected in goats on mixed dairy-goat/veal-calf farms (Bouma et al., 2003; Thompson et al., 2002). The loss of the agricultural sector was approximately 3.2 billion euros, and there were additional costs to other sectors, such as tourism, with the total expenditure being approximately 2.7 to 3.2 billion euros (Chanchaidechachai et al., 2021). Meanwhile, the distribution of FMD outbreaks in South America has changed over the years, with the most recent outbreaks being reported in Colombia in 2017 and 2018 (F. Gómez et

al., 2019), while no epidemics have been reported in Latin America since then, despite

Venezuela's absence of official international status for FMD (PANAFTOSA-OPS/OMS, 2019).

The official data from the World Organisation for Animal Health (WOAH) of more than

57 thousand outbreaks in 99 counties from 1996 until 2012 show that 68% of the cases were

associated with cattle, 22% with swine, and 21% with small ruminants and other species (Santos

et al., 2017). Even with strong evidence indicating that all susceptible species can drive large

FMD epidemics (Bertram et al., 2020; Tildesley et al., 2012) for example, the 2001 UK epidemic

was traced back to an infected Essex swine slaughterhouse (Davies, 2002) control measures and

surveillance programs have mostly been developed to target dissemination within cattle

populations, thus neglecting the role of other species in FMD transmission (Naranjo and Cosivi,

2013; Santos et al., 2017; Seymour et al., 2022; Singanallur et al., 2021).

It is worth noting that FMD pathogenesis and transmission dynamics are different,

including viral replication, persistence, incubation period, and potential to infect the same and/or

different hosts with different transmission probabilities, are different between species

(Alexandersen et al., 2003; Arzt et al., 2011; Moreno-Torres et al., 2022; Stenfeldt et al., 2016)

for example, pigs shed more viruses than cattle and sheep, which increases the transmission rate

when pigs are the more infectious host when compared with other domestic species (Brown et

al., 2022; Donaldson and Alexandersen, 2002; Moreno-Torres et al., 2022). Thus, it is pivotal

that such heterogeneity in the transmission dynamics is considered while modeling either within

or between-farm dissemination (Seymour et al., 2022). While, between-farm transmission

primarily occurs through direct contact among susceptible and infected animals (Alexandersen et

al., 2003; van Andel et al., 2021), field observations and experimental trials have demonstrated

the spread of the virus via indirect contact with fomites and long-distance transport of aerosols, a

process known as spatial transmission (Chakraborty et al., 2021; Guyver-Fletcher et al., 2021; Sellman et al., 2020; van Andel et al., 2021).

Mathematical models have been widely used to investigate epidemic propagation, although major technical and computation advancements have been achieved, in most cases models are simplified because of computational cost and/or lack of details about herd structure (e.g., number of heads, number of born alive) and animal movements. The most common simplification is to restrict the epidemiological models to a single species (Chanchaidechachai et al., 2021; Sseguya et al., 2022). Despite the different applications and efforts in modeling FMD, questions on measuring the epidemic trajectory and epidemic control strategies while considering heterogeneous transmission dynamics among the different susceptible species coexisting on the same farms remain outstanding (Seymour et al., 2022).

In this work, we proposed a novel multihost single-pathogen multiscale model with heterogeneous transmission dynamics and species-specific transmission coefficients. We present a quantitative assessment of the epidemiological role that each species plays in FMD dissemination, aiming to quantify transmission routes and the spatial distance of spread. Our simulations utilize population data including the birth and death data for the entire food-animal species population of the state of Rio Grande do Sul, Brazil. Finally, we examined the effectiveness of control and elimination actions according to the national FMD control plan (MAPA, 2020), which includes i) vaccination of uninfected animals; ii) depopulation of infected animals; iii) various between-farm movement restrictions; and iv) surveillance activities within control zones.

2.   Material and Methods

2.1 Data sources

We collected information from 415,364 farms officially registered in the state of Rio Grande do Sul (SEAPI, 2021). The data contained the population of cattle, buffalo, swine, sheep, and the number of farms, along with the daily between-farm animal movement and movements to slaughterhouses, from January 1st, 2018 until December 31st, 2020. Population and movement data of cattle and buffalo farms were combined into one species category, named hereafter "bovine". Similarly, we grouped sheep and goats into the "small ruminants" category. By analyzing the population data, we found 5,709 (1.37%) farms with missing geolocation, and these were then excluded from the analysis. More information about the population distribution by species is shown in Supplementary Material Figure S1. In Brazil, producers are required to report farming activities to the state animal health office once a year, and the report includes information about food animal production activities every twelve months. We utilized producer-reported data combined with the 2020 headcounts to classify farms as "active" if at least one food animal was present. Farms that were either declared inactive by the producer or had zero animals were considered inactive and not considered in this study. Therefore, our final active population included 409,655 farms.

2.2 Birth and death data

In the same way that producers are required to report the total number of heads, there are requirements to report the number of animals born alive and animal deaths, including natural deaths. We had access to the state database (SEAPI, 2021). Producers can report birth and death data any time throughout the year; however, reporting is mandatory at least once a year from January 1st until May 30th. We collected 256,504 individual records associated with birth and/or

death. The monthly description of births and deaths by species is depicted in Supplementary Material Figure S2. We found that 1.14% of the 409,655 farms had negative headcounts after the farm's population was computed, based on animal movements, births, and death records. To keep these farms in our simulations, any negative population values caused by movement or animal death were prevented by restoring the population values to their most recent positive record.

2.3 Movement data

Overall, from January 1st, 2018 until December 31st, 2020, the state database registered 1,634,940 unique between-farm and slaughterhouse movements. By analyzing the movement data, we found 181 movements with missing farm identification, 93,871 movements with the same farm identification at origin and destination, 51,490 movements to or from other states, and 112,834 movement records from or to farms with missing geolocation. After removing the movement data described above, the final database comprised 1,564,487 movements and 73,823,866 animals transported (Supplementary Material Figure S3 shows the movement data variations across the years).

2.4 Model formulation

We implemented a multihost single-pathogen coupled multiscale model to simulate FMD epidemic trajectories (Garira, 2018) and countermeasure effectiveness. This modeling work led to the development of a novel R package, MHASpread: A multihost animal spread stochastic multilevel model (version 0.1.0). MHASpread allows for explicit specification of species-specific transmission probability and latent and infectious period of disease infecting multiple species. At the within-farm dynamics level, we consider the entry and exit of animals given

between-farm animal movements, movements to slaughterhouses, births, and, deaths, for each species (Figure 1). The between-farm level dynamics are driven by the between-farm movements and spatial proximity.

2.5 Within-farm dynamics

The within-farm dynamics consist of mutually exclusive health states in which animals of each species (bovine, swine, and small ruminants) can only be in one compartment—susceptible (S), exposed (E), infectious, (I), and recovered (R)—per discrete time step, where:

(i) Susceptible: denotes animals that are not infected but susceptible.

(ii) Exposed: denotes animals that are exposed but not yet infected.

(iii) Infectious: denotes animals that are infected and can successfully transmit the infection.

(iv) Recovered: denotes animals who have recovered and are not susceptible.

Here, we also take into account the birth and death data described in the section above. The total population is represented as $N = S + E + I + R$, where the number of individuals within each compartment transitions from $S\beta \rightarrow E, 1/\lambda_1 \rightarrow I, 1/\lambda_2 \rightarrow R$ as follows:

$$\frac{dS}{dt} = u_{i,t,} - v_{i,t,} - \frac{\beta S_i I_i}{N_i} \tag{1}$$

$$\frac{dE}{dt} = \frac{\beta S_i I_i}{N_i} - v_{i,t,}O - \left(E_i \frac{1}{\lambda_1}\right) \tag{2}$$

$$\frac{dI}{dt} = \left(E_i \frac{1}{\lambda_1}\right) - \left(I_i \frac{1}{\lambda_2}\right) - v_{i,t,}I \tag{3}$$

$$\frac{dR}{dt} = I_i \frac{1}{\lambda_2} - v_{i,t,}$$
(4)

In short, birth is represented by the number of animals born alive $u_{i,t}$ entering into the S

compartment in farm i at a time t according to the day-to-day records; in the same vein,

$v_{i,t}$ represents the exit of the animals from any compartment due to death at time t (Figure 1).

The transition from E to I is driven by $1/\lambda_1$ and I to R by the $1/\lambda_2$ both drawn from the

distribution generated from each specific species according to the literature (Table 1). As the

infection progresses, animals transition into a recovered (R) state based on $1/\lambda_2$ drawn from the

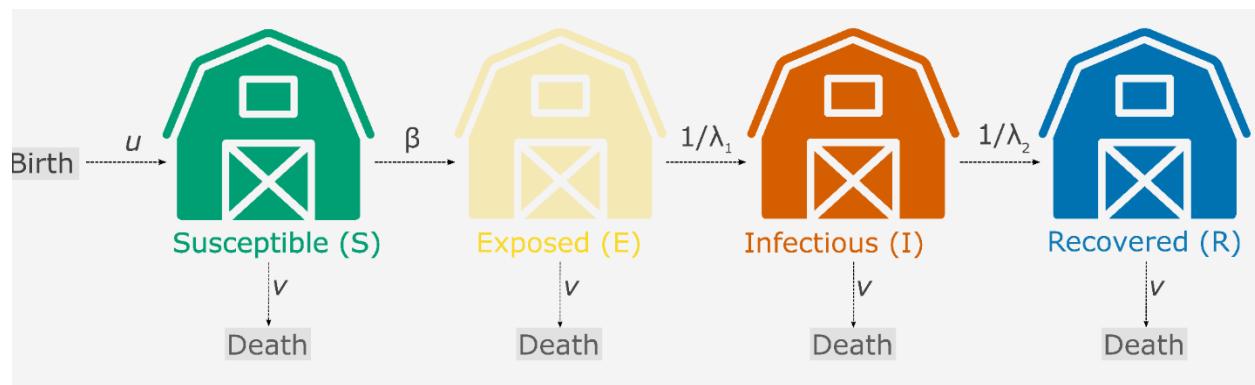infectious period, again because both λ_1 and λ_2 are specific to the host species (Table 2).

Figure 1. Within-farm dynamics. The framework represents the transition between

compartments, $S\beta \rightarrow E$, $1/\lambda_1 \rightarrow I$, $1/\lambda_2 \rightarrow R$, while the susceptible animals u are introduced

in S, and deaths v are removed from all compartments.

In the within-farm model dynamics, we assumed that populations were homogeneously

distributed and species were homogeneously mixed, where the frequency-dependent

transmission depends on the infected and the susceptible host species by using a species-specific

FMD transmission coefficient β (Table 1, Supplementary Material Figure S4, and Figure 2A).

Similarly, the transition from *E* to *I* and *I* to *R* occurs according to each species' parameters listed in the Table.

Table 1. The distribution of each host-to-host transmission coefficient (β) along with the parameter distribution per animal^{-1} day^{-1}.

Species	Species	Transmission coefficient (β)	References
Bovine	Bovine	Pert (0.018, 0.024, 0.056)	Calculated from the 2000-2001 FMD outbreaks in the state of Rio Grande do Sul (da Costa et al., 2022).
Bovine	Swine	Pert (0.018, 0.024, 0.056)	Assumed.
Bovine	Small ruminants	Triangular (0.020, 0.026, 0.031)	(Cabezas et al., 2021; Chis Ster et al., 2012)
Swine	Bovine	Pert (0.014, 0.044, 0.033)	(van Roermund et al., 2010)
Swine	Swine	Pert (0.014, 0.044, 0.033)	(Kinsley et al., 2018; van Roermund et al., 2010)
Swine	Small ruminants	Pert (0.014, 0.044, 0.033)	(van Roermund et al., 2010)
Small ruminants	Bovine	Pert (0.012, 0.031 0.065)	(Bravo de Rueda et al., 2014)
Small ruminants	Swine	Pert (0.006, 0.024, 0.09)	(Goris et al., 2009)
Small ruminants	Small ruminants	Pert (0.018, 00.24, 0.056)	Assumed

Table 2. The within-farm distribution of latent and infectious FMD parameters for each species.

FMD parameters	Species	Distribution parameters	Reference
Latent period, λ_1	Bovine	Weibull (a = 1.78, b = 3.97)	(Mardones et al., 2010)
	Swine	Log logistic (shape = 7.60; scale = 1.06)	(Moreno-Torres et al., 2022)
	Small ruminants	Pert (m = 3.96, a = 0, b = 13.98)	(Mardones et al., 2010)
Infectious period, λ_2	Bovine	Gamma (a = 3.97, b = 1.11)	(Mardones et al., 2010)
	Swine	Weibull (shape = 7.16; scale = 11.04)	(Moreno-Torres et al., 2022)
	Small ruminants	Pearson 5 (a = 6.19, b = 17.19)	(Mardones et al., 2010)

Note: The time unit is days.

2.6 Between-farm dynamics

For the farm-level dynamics, we consider two transmission pathways: i) between-farm animal movements and ii) spatial transmission. We utilized the number of unique movements (batches) and animals for each species to model the between-farm transmission while considering the current within-farm transmission dynamics status (Figure 2). Briefly, for each movement batch, we accessed the corresponding infection status from the available population at the farm of origin to draw the necessary animals to be transferred to the destination farm (Figure 2B). The animal movements to slaughterhouses were also taken into account in the same way as the between-farm moment; thus, we drew the number of animals to be removed from the current state of the system (Figure 2B).

2.7 Spatial transmission dynamics

Briefly, spatial transmission combines different transmission processes, such as airborne, shared fence lines, and sharing equipment, into one dynamic process. Furthermore, we used each farm's geolocation and grouped them within a grid-hexagon of size 0.76 km, representing an area of 503,516 m^2 (Supplementary Material Figure S5A). Farms within the same hexagon have the same spatial transmission probability (Figure 2C). The local spread was fitted using a spatial transmission kernel, where the likelihood of transmission decreases as a function of the distance between farms. The probability PE describes at time t the probability of a farm to become exposed, as follows:

$$PE = 1 - \prod_{1}^{i}(1 - \frac{I_i}{N_i}\varphi e^{-\alpha d_{ij}}) \qquad (5)$$

Where j represents the uninfected population and ad_{ij} is the distance between farm j and infected farm i to a maximum of 40 km from an infected farm(s). Because of the extensive literature about distance-based FMD dissemination and a previous comprehensive mathematical simulation study (Björnham et al., 2020) distances above 40 km were not considered. Here, $1 - \frac{I_i}{N_i}\varphi e^{-\alpha d_{ij}}$ represents the probability of transmission between farm i and j (scaled by infection prevalence in farm i, $\frac{I_i}{N_i}$) given the distance between farms in kilometers (Supplementary Material Figure S5B). The parameters φ and α control the shape of the transmission kernel, where $\varphi = 0.12$ is the probability of transmission when $d_{ij} = 0$, and $\alpha = 0.6$ control the steepness with which probabilities decline with distance (Boklund et al., 2013).
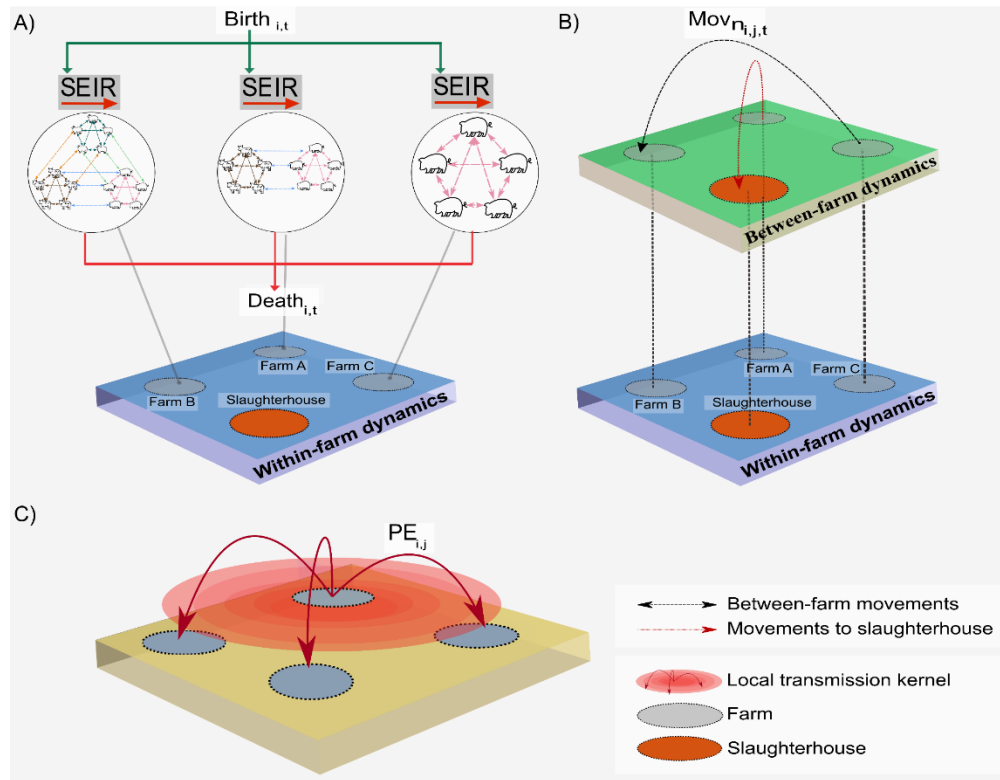
Figure 2. Schematic of state transitions of the within-farm and between-farm dynamics. A) Within-farm dynamics: green arrows indicate introduction events (births) into the susceptible (S) compartment at farm i at time t. Each circle shows a farm with its single or multiple species representing factorial host-to-host transition parameters ($\beta, \lambda_1, \lambda_2$), where the dashed color line represents the interaction within and between hosts. The red arrows represent the animal removed (death) regardless of their infection status. B) The between farm dynamics layer represents the number of animals moved (batches) n from the farm of origin i to a destination farm j, at time t (indicated by the black dash arrows). The animals moved to the slaughterhouse are removed from the simulation regardless of their infection status and are indicated by red dashed arrows. C) The spatial transmission distances.

2.8 Initial model conditions

We used 2018 population headcounts as the initial population condition. Because of the large number of farms, with 409,655 being considered prohibitively high computationally, we alternatively drew a sample of 15,721 farms to be used as initially infected locations. We used a multistage stratified sample design, in which strata were defined based on each municipality's animal population so that farms were sampled proportionally by species densities (Ziegel and Lohr, 2000). The sample size was calculated to maximize the sample size; thus, we used an expected prevalence of 50% with a level of significance of 95% and a margin of error of 1%.

We ran ten repetitions for each of the 15,721 sampled farms, and each repeat started at any date sampled between January 1st, 2018, and December 31st, 2020. In total, we analyzed 157,210 simulations. For each repeat, the infection started with one infected animal. In farms with more than one species, the seed infection priority order was bovine, swine, and small ruminants. All farms were assumed to be fully susceptible to FMD infection since vaccination has been suspended in Rio Grande do Sul since May 2021 (da Costa et al., 2022).

2.9 Local sensitivity analysis

We used a combination of Latin hypercube sampling (LHS), developed by McKay (Mckay et al., 2000), and the statistical partial rank correlation coefficient (PRCC) technique to perform a local sensitivity analysis. LHS is a stratified Monte Carlo sampling without replacement technique that gives unbiased estimates of modeling output measures subject to combinations of varying parameters. The PRCC can be used to classify how the output measures are influenced by changes in a specific parameter value, while linearly discounting the effects of the other parameters (Marino et al., 2008). We selected the parameters and the distribution listed in Tables 1 and 2 with the size of the population in each host species (bovine, swine, and small ruminants)

ranging from ten to 1,000 as input model parameters. In total 18 parameters were used to classify the monotone relation with our input variables by using a total of infected animals to classify the sensitivity. The inputs include one farm where the initial conditions varied across 10,000 simulations over the LHS sample space. Here, a positive PRCC has a positive relationship with the number of infected animals, whereas a negative PRCC value has an inverse relationship with this output measure; however, larger PRCC values do not necessarily indicate more important parameters (Teboh-Ewungkem and Ngwa, 2021).

3.1 Evaluation of control and eradication scenarios

We simulated FMD epidemic trajectories for up to 20 days. Based on the historic FMD outbreaks in Brazil and in consultation with animal health officials, control actions were started at ten and 20 days of silent FMD dissemination. Thus, the initial number of infected farms at ten and 20 days were compared with the three alternative control scenarios with a predefined baseline control scenario based on the national FMD response plan (MAPA, 2022, 2020), described below.

Baseline control scenario: This scenario incorporated the national FMD control and eradication plan (MAPA, 2022), which included the following measures: i) depopulation of infected farms, ii) vaccination of uninfected farms, iii) animal movement standstill for 30 days, iv) three distinct control zones around infected farms: 3 km (infected zone), 7 km (buffer zone), and 15 km (surveillance zone) (Supplementary Material Figure S6). In the infected zones, infected farms are depopulated as FMD is detected, while vaccination is implemented stating in farms within infected zones. If vaccine doses are still available after vaccinating the farms in the infected zones then farms in buffer zones are vaccinated. Surveillance activities are defined as

clinical examinations. In our simulation, all farms within control zones were visited every three days. Contact tracing of farms with direct links to infected farms for the past 30 days underwent surveillance and, if positive, the animals detected in these farms are moved into the infected compartment. Here, we also take into consideration the state budget as follows: i) four is the maximum number of farms that can be depopulated per day, and ii) the maximum number of animals vaccinated per day is 5,000; both assumptions are based on the state's maximum personnel and equipment capacity (personal communication, animal health official working group). We also included a delay in the start of vaccination of seven days after the first case was detected; vaccination was assumed to be effective instantaneously, and thus vaccinated animals were moved into the recovered compartment (R). In addition, we assumed that i) surveillance was 100% sensitive for FMD detection and, ii) we also assumed 100% compliance with the 30-day animal movement standstill.

In addition to the baseline control scenario, three alternative scenarios were considered:

Scenario 1: Vaccination & depopulation. Depopulation of eight infected farms per day and vaccination of 10,000 animals per day.

Scenario 2: Depopulation only. Depopulation of eight infected farms per day.

Scenario 3: Enhanced vaccination & depopulation. Depopulation of 12 infected farms per day and vaccination of 15,000 animals per day.

3.2 Model outputs

Our simulations tracked the number of animals and farms in each health compartment throughout the daily time steps. We also utilized the epidemic trajectories to calculate the geodesic distances between the seeded infections and secondary cases. In addition, we elucidated

the probability of distance-dependent transmission by calculating the cumulative empirical spatial distribution. By tracing the average of secondarily infected animals resulting from each transmission route, we estimated the contribution of between-farm movement and spatial transmission in infecting each species; here, we present the average contribution for each route along with credible intervals estimated by using an equal-tailed interval method (Lecoutre, 2011). We also determined the volume of animals and farms within control zones at ten and 20 days post-FMD dissemination.

In collaboration with Brazilian animal health officials, based on the local animal health capacity control action was further remained before simulations were run. Briefly, we used the ten and 20 days FMD epidemics as the initial conditions, from which we first removed simulations with more than 400 infected farms because such large epidemics exceeded the maximum capacity of the state of Rio Grande do Sul (state animal health official, personal communication, 2022). We applied the control action over the remaining simulations (99.51%). We further classified control scenarios as successful or unsuccessful FMD elimination. When no more infected farms were present in simulations the repeat was stopped and classified as successful. While unsuccessful simulating were we are the repeats in which either the number of infected farms was above 450 infected farms or when the time since control actions were deployed exceeded 100 days. Finally, we also kept track of the number of days control interventions were applied.

The software used in the development of MHASpread, graphics, and maps was the R statistical software v. 4.1.1 (R Core Team, 2021) with RStudio editor using the following packages: sampler (Baldassaro, 2019), tidyverse (Wickham et al., 2019), sf (Pebesma, 2018), brazilmaps (Prado Siqueira, 2021), doParallel (Corporation and Weston, 2022a), doSNOW

(Corporation and Weston, 2022b), RSQLite (Muller et al., 2021), EpiContactTrace (Noremark and Widgren, 2014), and lubridate (Grolemund and Wickham, 2011).

3. Results

3.1 Farms and animal-level FMD temporal dynamics

Of 15,721 seeded infections, 10,473 simulations started in cattle farms, 5,179 in swine farms, and 69 in small ruminant farms, while 4,702 farms (29%) had multiple species. Examining the epidemic trajectories at 20 days post-seeded infection, we estimated a median of 15 (IQR: 5-41) infected animals, of which 12 (IQR: 4-32) were bovine, 5 (IQR: 2-12) were swine, and 1 (IQR: 1-2) was small ruminant (Supplementary Material Table S1 and Figure S7). The animal-level infection distribution of each compartment at ten and 20 days is shown in Supplementary Material Table S1.

The FMD epidemic distribution at the farm level at 20 days was highly variable; the median number of infected farms was 8 (IQR: 3-22), of which 7 (IQR: 3-18) were bovine farms, 3 (IQR: 1-6) were swine farms, and 1 (IQR: 1-1) was a small ruminant farm (Figure 3). While we observed large-scale epidemics with up to 2,197 infected farms, these rare events were outside the 95% credibility interval (Figure 3). The farm-level infection distribution at ten and 20 days post seeded infection is available in Supplementary Material Table S2.
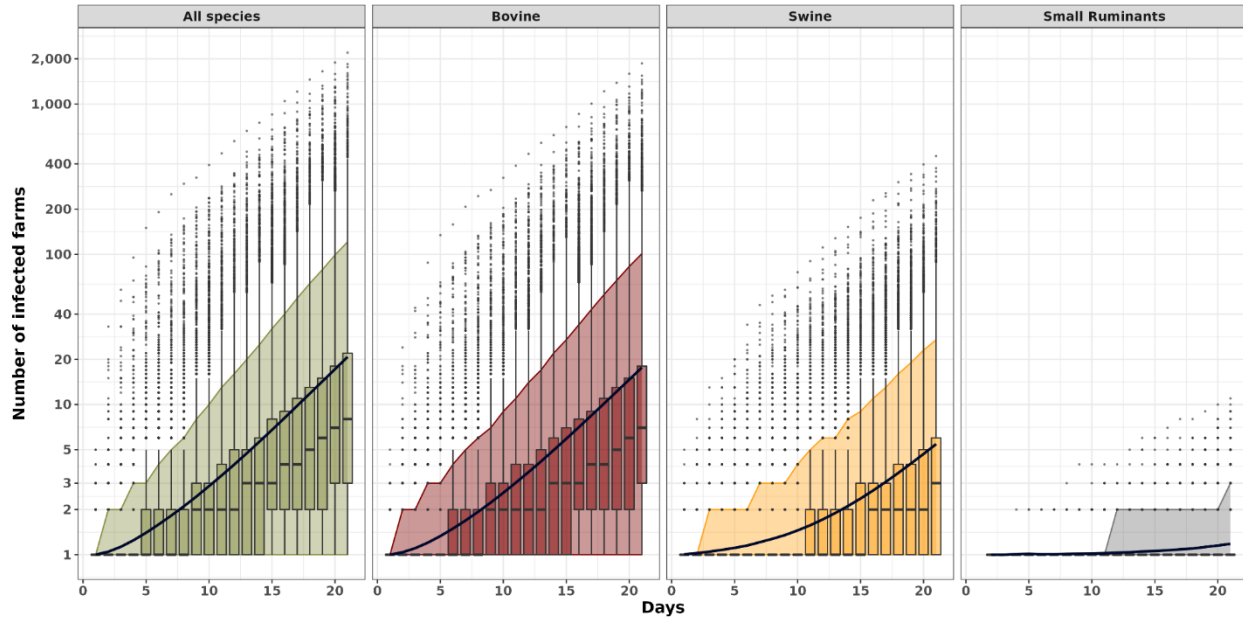
Figure 3. Distribution of the daily number of infected farms. Boxplots with outliers for the number of infected farms. The colored background area represents the 95% credible interval for the daily number of infected farms. The y-axis is on a log10 scale.

3.2 Contribution of transmission routes

Evaluating the contribution of the between-farm and spatial transmission routes, we demonstrated that overall, for the first 17 days of FMD dissemination, the main transmission route was animal movements, with an average of 4.9 (CI: 1-23) newly infected animals, while at 20 days, spatial transmission was by far the dominant route, with a daily average of 11 (CI: 1-95.6) newly infected animals. When we examined transmission contributions by species, at ten days bovine infection shifted from spreading via animal movement to spatial transmission. While new bovine infections at 20 days occurred predominantly by spatial transmission, we estimated an average of 10.7 (CI: 1-57) new infections, while animal movement represented an average of 4.5 (CI: 1-32) new infections. For swine, animal movement was undoubtedly the most important

route throughout the simulation period; at 20 days, it generated on average 11.4 (CI: 1-123) newly infected pigs, while spatial transmission produced on average 3.1 (CI: 1-90) of newly infected pigs. Finally, for small ruminants, both routes appear to contribute at a similar rate (Figure 4). The summary statistics of each route at ten and 20 days are available in Supplementary Material Table S3.
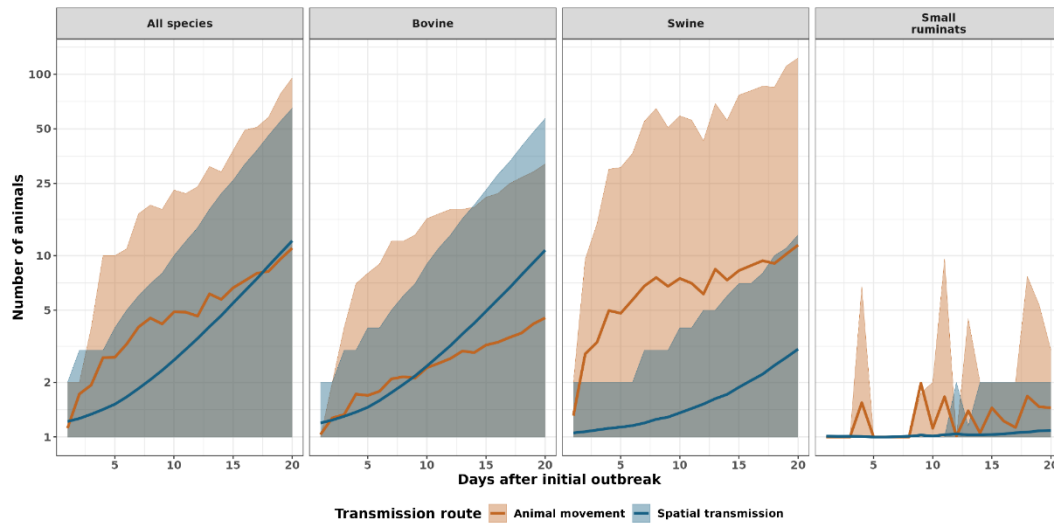

Figure 4. FMD transmission via between-farm movement or spatial transmission. The x-axis represents the number of days after seeded FMD infection. The y-axis (represented on a log10 scale) shows the number of newly infected animals, the solid line represents the average, and the colored background represents the 95% credible interval distribution.

3.3 Spatial transmission dynamics

Of the 15,721 seeded infections, we measured the distance between 386,043 simulations that generated secondary infection. The median distance between seeded infection and secondary infections was 5.77 km (IQR: 1-10.29 km). Our simulations also captured long-distance spreads at 100 km and 500 km, while the maximum dispersal was at 695.40 km (Figure 5A). As noted in

Figure 5B, the probability of infection decreased by 11% when we compared one km with 20 km.
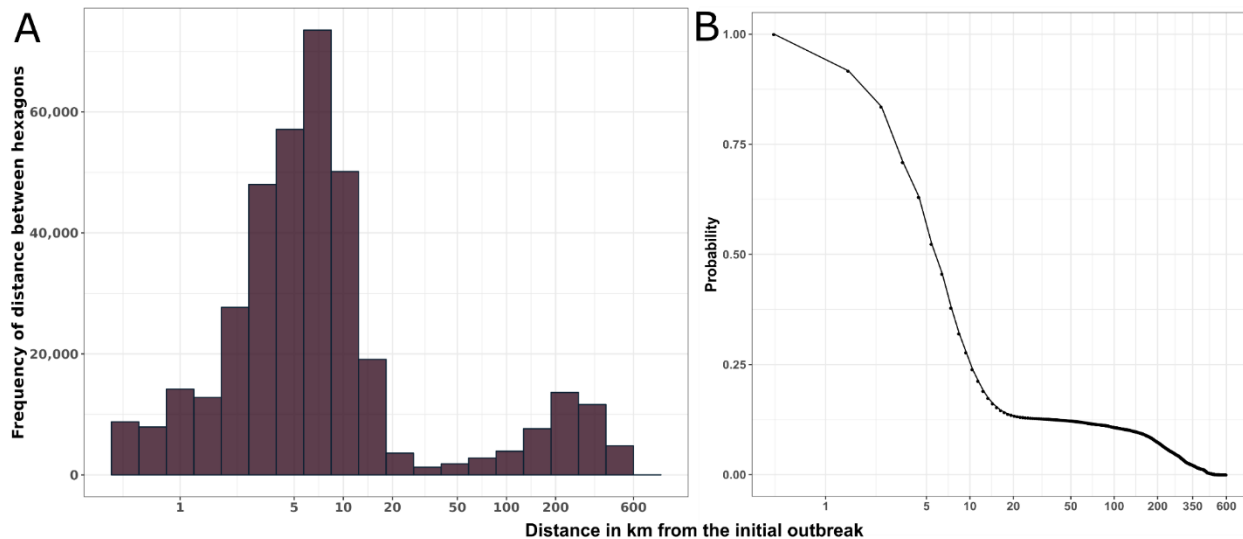

Figure 5. Distribution of the cumulative epidemic distances. A) Frequency histogram of distances from seeded infection and secondary infections. B) Empirical cumulative distribution function (1-ECDF) probability of distances from the initial outbreak. Both x-axes are a log10 scale.

3.4 Sensitivity analysis

Given the lack of FMD outbreak data model calibration we evaluated the sensitivity of 18 model parameters. Parameter values varied from -0.17 to 0.24, which indicates a limited influence on the number of simulated secondary animal infections. While λ_1 of all host species showed a negative influence while β of small ruminants to swine, β small ruminants to bovine, β small ruminants to small ruminants, and λ_2 of small ruminants were positively correlated, the full results are depicted in the Supplementary Material Figure S10.

3.5 Effectiveness of control strategies

We calculated the number of animals and farms within control zones. On Day 20 of silent FMD dissemination, the total number of animals and farms within infected zones had a median of 8,660 (IQR: 308-53,783) animals and 1,785 (IQR: 583-4,804) farm; in buffer zones, the median was 77,679 (IQR: 2,408-384,439) animals and 12,303 (IQR: 4,357-30,900) farms; and within surveillance zones, the median was 369,541 (IQR: 9,599-1,460,202) animals and 50,148 (IQR: 19,295-105,943) farms (Figure 6 and Supplementary Material Figure S8 for the animal-level distributions). Animal-level results at ten days are shown in Supplementary Material Table S4 and Supplementary Material Figure S9; at farm-level, in Supplementary Material Figure S11 and Table S5.
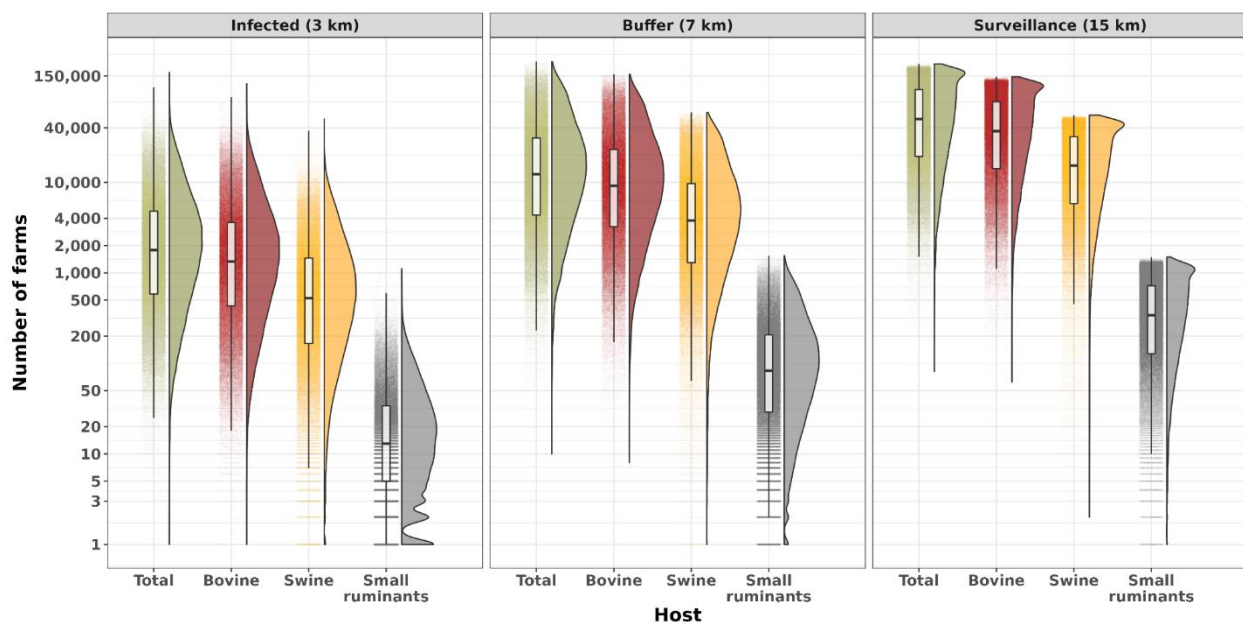

Figure 6. The distribution of farms within control zones at 20 days from the initial infection. The y-axis shows the number of animals within infected zones, buffer zones, and surveillance on a log10 scale. The left-side box plots include outliers and the right-size density distribution.

We demonstrated that the number of days necessary for successfully eradicating FMD depended on the number of secondary infections at 20 days and the duration of control actions (Figure 7). The baseline control scenario fade out 93.4% of the epidemics with a median of 9 (IQR: 3-23, max: 221) infected farms, while scenario one, which has twice the depopulation and vaccination of the baseline scenario, eliminated 97,8% of simulated epidemics with a median of 10 (IQR: 4-26, max: 223) infected farms. Scenario two eliminated (depopulation only) 78.4% of simulated epidemics, stopping mostly small-scale epidemics with a median of 7 (IQR: 3-14, max: 74) infected farms. Scenario three, which had three times more depopulation and vaccination than the baseline control scenario, was enough to fade out 98.3% of epidemics with a median of 10 (IQR: 4-26, max: 248) initially infected farms (Figure 7 and Supplementary Material Table S6). Examining epidemics in which control actions were unsuccessful, scenario two (depopulation only) was the least effective scenario; it was unable to contain epidemics with a median of 61 (IQR: 43-93, max: >=400) initially infected farms. The baseline control scenario was unsuccessful in eliminating simulations with a median of 116 (IQR: 82-161, max:>=400) infected farms, while scenarios one and three did not stop epidemics with medians of 183 (IQR: 152-244, max: >=400) and 203 (IQR: 170-264, max: >=400) infected farms, respectively (Figure 7).
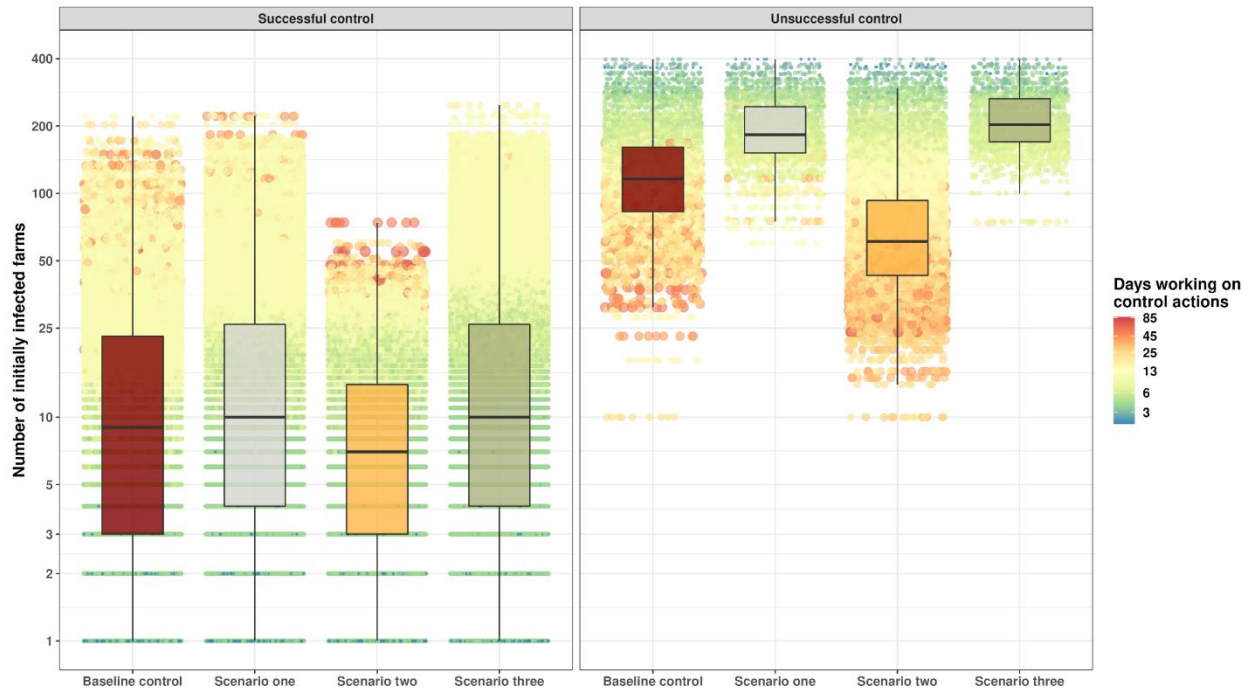
Figure 7. The distribution of FMD epidemics that were successfully and unsuccessfully halted under four control and eradication scenarios 20 days after the initial seeded infection. The box plot shows the distribution of secondarily infected farms at 20 days, and the background scattered plot shows individual stochastic simulations in which color represents the number of days that control and eradication measures were applied. The y-axis is represented in the log10 scale.

Of the successfully halted epidemic shown in Figure 7, the baseline control and scenario two stamped all epidemics in 99 days. Scenarios one and three took 84 and 54 days, which means 15 and 45 fewer days to eliminate simulated epidemics when compared with the baseline control scenario (Figure 8).
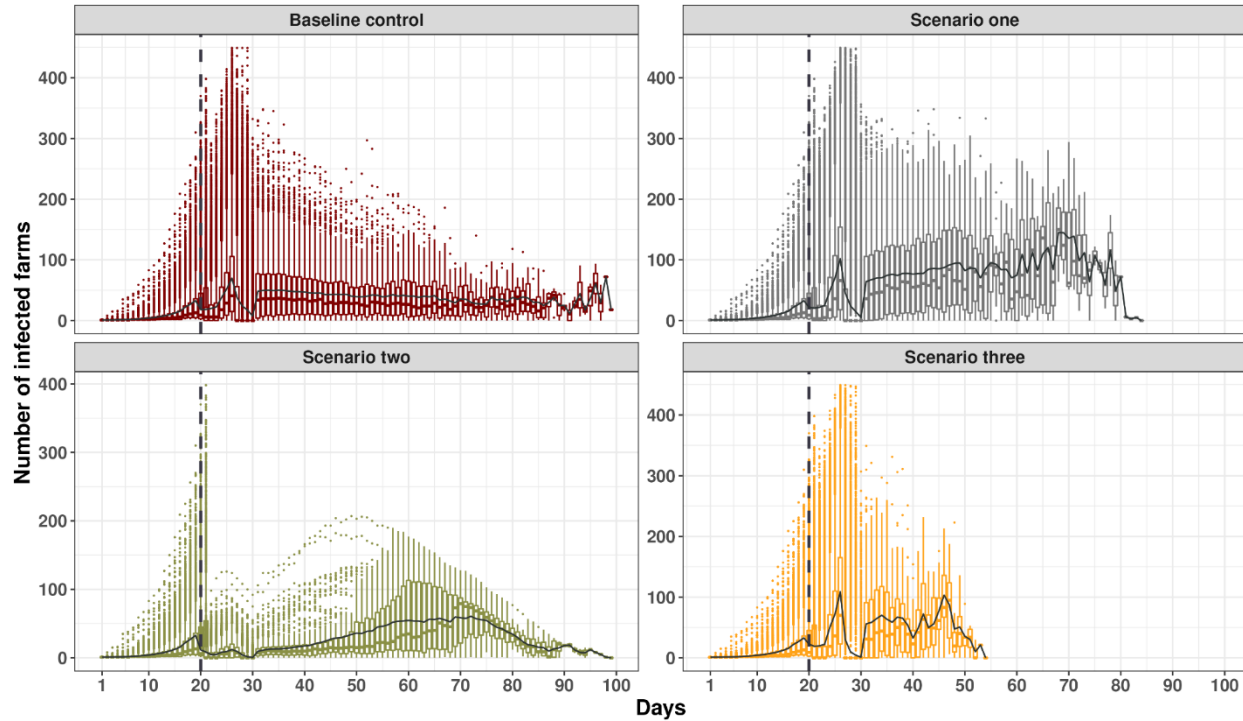
Figure 8. The average number of days to successfully eliminate FMD epidemics. The vertical dashed line marks the 20 days of silent FMD spread and the start of control actions. The solid black line represents the average daily infected farms. In addition, we simulated control actions starting 10 days after seeding, and the initial infection is described in greater detail in the Supplementary Material Section "Effectiveness of control actions started 10 days after initial simulated infection."

4. Discussion

We developed an SEIR multispecies stochastic model that explicitly incorporates species-specific transmission coefficients. However, even by including different species interactions, bovines remained the most infected species followed by swine and small ruminants. The animal movement was the most effective transmission route for the first ten days for all species infections, after which bovine infection occurred predominantly by spatial transmission, while

for swine, the between-farm movement was the most important route for the first 20 days. Our results also demonstrated that most (74.7%) secondary cases spread to farms within ten km of the initial seeded infection. We also demonstrated that the baseline control scenario and alternative scenarios were sufficient to eradicate the majority of epidemics within 100 days.

Based on the 2018/2020 population and the between-farm animal movement patterns in the state of Rio Grande do Sul, we demonstrated that FMD is likely to disseminate between different production systems, e.g., bovine to swine and vice-versa, regardless of which species is infected first (Supplementary Material Figure S14). Our results showed that the preferred route of infection was not the same across species, a phenomenon that has been demonstrated previously (McReynolds et al., 2014; Probert et al., 2018; Sanson et al., 2014; Ward et al., 2009). We demonstrated that until day 17, if we consider all species together, between-farm movement was the predominant dissemination route, whereas, for bovines, spatial transmission became the preferred transmission route at day ten. The demonstrated predominance of spatial transmission later in the epidemic could be explained at least to some degree by spread across short to mid distances in some areas of the state of Rio Grande do Sul characterized by cool temperatures and high humidity, which are known to favor virus survival rates (Björnham et al., 2020; Chanchaidechachai et al., 2021; Green et al., 2006). More importantly, based on the high connectivity of bovine farms in some municipalities described earlier (Cardenas et al., 2022), the initial peak in bovine infection could be explained by the movement of animals, while the flip toward spatial transmission could have been facilitated when secondary cases spread into areas densely populated with up to 12.23 km^2 farms (Cardenas et al., 2022) These densely populated areas coincide with our model simulation in which control actions were not sufficient to stamp out large-scale epidemics (Supplementary Material Figure S15). Even though our modeling work

considered the main transmission routes, data regarding other important indirect transmission routes were not considered, e.g., fomites and transportation vehicles (Paton et al., 2018; Rossi et al., 2017) future iterations could include these additional routes. Importantly, when we evaluated swine infection the pig movements were by far the most relevant transmission pathway in our study and elsewhere (Andraud et al., 2022; Machado et al., 2021; Shimizu et al., 2020). For small ruminant dynamics, our results did not clearly uncover any dominant transmission route; however, even though small ruminants did not contribute significantly to FMD transmission, their contribution was not null. Overall, our result suggests the need for the enhancement of FMD control strategies by also including swine and small ruminants. Prioritizing control interventions related to traceability early in an FMD epidemic, especially in the first ten days is likely to increase the chances of finding more secondary infections, whereas enhancing surveillance activities within control zones should be prioritized if FMD is detected after ten days of silent dissemination.

Based on the estimated number of animals and farms within control zones at 20 days of FMD dissemination, and assuming that three qualified veterinarians can vaccinate approximately 1,000 animals per day (personal communication, animal health officials), we estimated the daily need to be 160 veterinarians to oversee an average of 4,222 farms within infected zones and approximately 53,434 vaccine doses if all species are vaccinated or 21,640 without vaccinating swine. If vaccination is also deployed to buffer zones, 320,223 doses of vaccine and 961 veterinarians would be required to vaccinate all animals, or 137,046 doses and 411 veterinarians without vaccinating swine. Similar modeling work in Denmark has predicted an average of 22 epidemics that last for 34 days and would need 123 veterinarians (Boklund et al., 2017). It is important to note that the estimations provided in the current study were based on the median

epidemic sizes of the ones recorded in the UK and Argentina (Anderson, 2002; Perez et al., 2004), which included large-scale epidemics with up to 398 secondary infections, thus much larger than the scenarios in Denmark. We remark that if such large-scale FMD epidemics occur in the state of Rio Grande do Sul, the resources necessary—trained animal health officials, adequate vaccine stockpiles, and supplies for depopulation—would be beyond the local capacities, and FMD would become endemic. Hence, future work should focus on estimating not only the number of animal health officials but also administrative, direct, and indirect costs, including large-scale epidemic scenarios. In addition, this new transmission modeling study should include extended delays in disease detection, the necessary downtime between farm visits, and other relevant logistical roadblocks linked to controlling and eliminating large-scale epidemics (Anderson, 2002).

Several modeling works have demonstrated the effectiveness of the combination of vaccination with depopulation in FMD elimination (Capon et al., 2021; Dürr et al., 2014; Sanson et al., 2017), with some exceptions in highly dense livestock areas, such as in the Netherlands, where vaccination combined with ring culling was not sufficient (Boklund et al., 2013). Among the simulated scenarios, implementing vaccination in conjunction with depopulation was always more effective when compared with depopulation alone (Figures 7 and 8). One potential explanation could be related to spatial transmission being the predominant transmission route after 20 days, when most transmission events occurred within a median of up to seven km from infected farms, which encompass infected zones. Even though we demonstrated that the use of the depopulation scenario alone exhibited a lower rate of successful FMD elimination, it was capable of eliminating small-scale epidemics (maximum of 74 infected farms). While less successful if the region decides against vaccinating (da Costa et al., 2022), one would expect the

region to regain FMD-free status sooner if compared with using vaccination (Geale et al., 2015).

From our alternative control scenarios, scenario three was the most aggressive, considering that

the state would be able to depopulate 12 farms and 15,000 farms vaccinated per day;

unfortunately, it was still not sufficient to eliminate large-scale epidemics (more than 400

infected farms at 20 days of silent FMD dissemination). Ultimately, we estimated the need to

depopulate 120 farms and vaccinate 25,000 animals within seven days to eliminate all simulated

epidemics, which seems extremely unrealistic given the current state of Rio Grande do Sul

staffing and available resources. Thus, we reach the same conclusion as the modeling work done

in Austria, which found that the number of animal health officials for surveillance and control

activities would need to be doubled to allow proper large-scale epidemic management (Boklund

et al., 2017; Marschik et al., 2021; Sanson et al., 2021). Finally, our model provides guidance to

Brazilian policy-makers, and our results are the first to provide rules of thumb based on the

number of infected farms, to choose whether to deploy vaccination. We demonstrated that in

situations in which the number of secondary cases varies between three and 23, the baseline

control scenario is likely to be sufficient when applied for 100 days. However, we highlight that

a small number of simulations with fewer than 50 infected farms at 20 days of dissemination that

were not successfully controlled by the baseline control scenario. Thus, it is important to

consider the profile of infected farms, such as location and the size of the farm's contact network

(Cardenas et al., 2022) along with simulated results to make field-level decisions. Finally, we

remark that as described earlier, we assume full compliance with all associated surveillance

actions and movement restrictions; thus, the results should be interpreted with this in mind.

5. Limitations and further remarks

We identify a number of limitations, mostly related to assumptions made in the simulated FMD control scenarios. We utilized the FMD outbreak in 200-2001 and published data to select transmission parameters that could have an impact on final simulations. Our sensitivity analysis of population, latent and infection periods, and β of each species did not significantly affect the final number of infected animals. Thus, the results suggest that our model has an acceptable level of robustness.

We assume perfect compliance with between-farm movement restrictions for infected farms and farms directly linked to infected farms, and movement restrictions within control zones, while also assuming that the disposal of depopulated animals eliminated any possibility of further dissemination. Nevertheless, there are uncertainties about the implementation of control measures, and future work could include delays in response times. Additionally, given the volume of vaccines necessary to vaccinate all animals within infected and buffer zones, further work should consider restricting vaccination to each species, thus allowing for benchmarking and better estimation of vaccine stockpiles (Capon et al., 2021; Dürr et al., 2014; Roche et al., 2015). Another limitation was the assumption of instantaneous vaccination efficacy; future work should consider a variation in vaccination waning (Ringa and Bauch, 2014).

It is worth noting that FMD virulence, infectivity, and transmission vary among strains (Arzt et al., 2019; Paton et al., 2018). Even though the most recent outbreaks in the state of Rio Grande do Sul were caused by serotypes O and A (da Costa et al., 2022), we cannot rule out the chances of other strains being introduced and exhibiting different dissemination patterns. Future work could include transmission scenarios with strains in circulation across the globe (Mahapatra and Parida, 2018).

To our knowledge, this is the first FMD transmission model developed for Latin American countries. While FMD transmission models have previously included multiple species in their transmission dynamics (Björnham et al., 2020; Boklund et al., 2013; Dürr et al., 2014; Roche et al., 2015), to the author's knowledge, none have explicitly considered the heterogeneous transmission rates of each species. Another unique feature of our model is that the estimation of successful and unsuccessful epidemics fade out while also assessing the maximum number of outbreaks and the number of days needed to complete FMD elimination. Thus, we provided rules of thumb for the four main control and eradication strategies, by estimating the number of secondary infections that the simulated scenarios are capable of stamping out. Our results offer scientific support to decision-makers.

In addition, rather than selecting a limited number of farms to seed infection, our modeling approach considers an honest representation of the entire population at risk. While our approach is more expensive, our results provide policy-makers with an overview of all possible introduction scenarios, which is important because it is nearly impossible to predict where FMD may resurface. Finally, our model can also provide a distribution of expected FMD epidemics for any current or future control actions listed in the Brazilian control and elimination plan. Nevertheless, because our results are based on population and between-farm movement data from Rio Grande do Sul, the interpretation of our findings should not be extrapolated to other Brazilian states. However, since the MHASpread model infrastructure is highly flexible, upon the availability of the necessary population data and animal movement data, MHASpread can be easily extended to any other Brazilian state and considered in other Latin American countries.

6. Conclusion

We demonstrated that 20 days of silent FMD dissemination resulted in a median of eight, ranging between three and 22 secondary infected farms. Early detection was pivotal to the success of FMD elimination, and we demonstrated that the deployment of depopulation alone was effective if applied to simulations with up to 22 infected farms. However, large-scale epidemics simulated required the depopulation of 100 farms and vaccination of 25,000 animals per day to eliminate 100% of the simulated outbreaks. We showed that for the first 17 days of epidemics, the movement of animals was predominated in the overall dissemination, however, with significant differences in the dissemination of bovine and swine infections. In whichever species FMD was first introduced, the median distance spread was within the range of control zones, from one to ten km. We have also shown that the baseline control scenario, based on the Brazilian response plan, was sufficient to stamp out 93.83% of all epidemics within 100 days of the deployment of countermeasure actions. Ultimately, our model projections are available to the local animal health official along with the necessary software. Thus, our model can be used as a policy tool not only for future FMD response through computer-based preparedness drills and capacity building but also ultimately during an emergency response by providing rules of thumb generated from simulated control scenarios.

Acknowledgments

Credit authorship contribution statement

NCC and GM conceived the study. NCC and GM participated in the design of the study. FPNL coordinated the data collection. NCC conducted data processing and cleaning designed the model and simulated scenarios with the assistance of GM. NCC and GM designed the computational analysis. NCC conducted the formal coding. GM and NCC wrote and edited the manuscript. All authors discussed the results and critically reviewed the manuscript. GM secured the funding.

Declaration of interest

All authors confirm that there are no conflicts of interest to declare.

Funding

References

Alexandersen, S., Zhang, Z., Donaldson, A.I., Garland, A.J.M., 2003. The Pathogenesis and Diagnosis of Foot-and-Mouth Disease. J. Comp. Pathol. 129, 1–36. https://doi.org/10.1016/S0021-9975(03)00041-0

Anderson, I., 2002. Foot and mouth disease: Lessons to be learned inquiry report HC888. Lond. Station. Off.

Andraud, M., Hammami, P., H. Hayes, B., A. Galvis, J., Vergne, T., Machado, G., Rose, N., 2022. Modelling African swine fever virus spread in pigs using time-respective network data: Scientific support for decision makers. Transbound. Emerg. Dis. tbed.14550. https://doi.org/10.1111/tbed.14550

Arzt, J., Branan, M.A., Delgado, A.H., Yadav, S., Moreno-Torres, K.I., Tildesley, M.J., Stenfeldt, C., 2019. Quantitative impacts of incubation phase transmission of foot-and-mouth disease virus. Sci. Rep. 9, 2707. https://doi.org/10.1038/s41598-019-39029-0

Arzt, J., Juleff, N., Zhang, Z., Rodriguez, L.L., 2011. The Pathogenesis of Foot-and-Mouth Disease I: Viral Pathways in Cattle: Foot-and-Mouth Disease Pathogenesis in Cattle. Transbound. Emerg. Dis. 58, 291–304. https://doi.org/10.1111/j.1865-1682.2011.01204.x

Baldassaro, M., 2019. sampler: Sample Design, Drawing & Data Analysis Using Data Frames.

Bertram, M.R., Yadav, S., Stenfeldt, C., Delgado, A., Arzt, J., 2020. Extinction Dynamics of the Foot-and-Mouth Disease Virus Carrier State Under Natural Conditions. Front. Vet. Sci. 7, 276. https://doi.org/10.3389/fvets.2020.00276

Björnham, O., Sigg, R., Burman, J., 2020. Multilevel model for airborne transmission of foot-and-mouth disease applied to Swedish livestock. PLOS ONE 15, e0232489. https://doi.org/10.1371/journal.pone.0232489

Boklund, A., Halasa, T., Christiansen, L.E., Enøe, C., 2013. Comparing control strategies against foot-and-mouth disease: Will vaccination be cost-effective in Denmark? Prev. Vet. Med. 111, 206–219. https://doi.org/10.1016/j.prevetmed.2013.05.008

Boklund, A., Mortensen, S., Johansen, M.H., Halasa, T., 2017. Resource Estimations in Contingency Planning for Foot-and-Mouth Disease. Front. Vet. Sci. 4, 64. https://doi.org/10.3389/fvets.2017.00064

Bouma, A., Elbers, A.R.W., Dekker, A., de Koeijer, A., Bartels, C., Vellema, P., van der Wal, P., van Rooij, E.M.A., Pluimers, F.H., de Jong, M.C.M., 2003. The foot-and-mouth disease epidemic in The Netherlands in 2001. Prev. Vet. Med. 57, 155–166. https://doi.org/10.1016/S0167-5877(02)00217-9

Bravo de Rueda, C., de Jong, M.C., Eblé, P.L., Dekker, A., 2014. Estimation of the transmission of foot-and-mouth disease virus from infected sheep to cattle. Vet. Res. 45, 58. https://doi.org/10.1186/1297-9716-45-58

Brown, E., Nelson, N., Gubbins, S., Colenutt, C., 2022. Airborne Transmission of Foot-and-Mouth Disease Virus: A Review of Past and Present Perspectives. Viruses 14, 1009. https://doi.org/10.3390/v14051009

Cabezas, A.H., Sanderson, M.W., Volkova, V.V., 2021. Modeling Intervention Scenarios During Potential Foot-and-Mouth Disease Outbreaks Within U.S. Beef Feedlots. Front. Vet. Sci. 8.

Capon, T.R., Garner, M.G., Tapsuwan, S., Roche, S., Breed, A.C., Liu, S., Miller, C., Bradhurst, R., Hamilton, S., 2021. A Simulation Study of the Use of Vaccination to Control Foot-and-Mouth Disease Outbreaks Across Australia. Front. Vet. Sci. 8, 648003. https://doi.org/10.3389/fvets.2021.648003

Cardenas, N.C., Sykes, A.L., Lopes, F.P.N., Machado, G., 2022. Multiple species animal movements: network properties, disease dynamics and the impact of targeted control actions. Vet. Res. 53, 14. https://doi.org/10.1186/s13567-022-01031-2

Chakraborty, D., Başağaoğlu, H., Winterle, J., 2021. Interpretable vs. noninterpretable machine learning models for data-driven hydro-climatological process modeling. Expert Syst. Appl. 170. https://doi.org/10.1016/j.eswa.2020.114498

Chanchaidechachai, T., de Jong, M.C.M., Fischer, E.A.J., 2021. Spatial model of foot-and-mouth disease outbreak in an endemic area of Thailand. Prev. Vet. Med. 195, 105468. https://doi.org/10.1016/j.prevetmed.2021.105468

Chis Ster, I., Dodd, P.J., Ferguson, N.M., 2012. Within-farm transmission dynamics of foot and mouth disease as revealed by the 2001 epidemic in Great Britain. Epidemics 4, 158–169. https://doi.org/10.1016/j.epidem.2012.07.002

Corporation, M., Weston, S., 2022a. doParallel: Foreach Parallel Adaptor for the "parallel" Package.

Corporation, M., Weston, S., 2022b. doSNOW: Foreach Parallel Adaptor for the "snow" Package.

da Costa, J.M.N., Cobellini, L.G., Cardenas, N.C., Groff, F.H.S., Machado, G., 2022. Assessing epidemiological parameters and dissemination characteristics of the 2000 and 2001 foot-and-mouth disease outbreaks in Rio Grande do Sul, Brazil. bioRxiv 2022.05.22.492961. https://doi.org/10.1101/2022.05.22.492961

Davies, G., 2002. The foot and mouth disease (FMD) epidemic in the United Kingdom 2001. Comp. Immunol. Microbiol. Infect. Dis. 25, 331–343. https://doi.org/10.1016/S0147-9571(02)00030-9

Donaldson, A.I., Alexandersen, S., 2002. Predicting the spread of foot and mouth disease by airborne virus: -EN- -FR- -ES-. Rev. Sci. Tech. OIE 21, 569–575. https://doi.org/10.20506/rst.21.3.1362

Dürr, S., Fasel-Clemenz, C., Thür, B., Schwermer, H., Doherr, M.G., Dohna, H. zu, Carpenter, T.E., Perler, L., Hadorn, D.C., 2014. Evaluation of the benefit of emergency vaccination in a foot-and-mouth disease free country with low livestock density. Prev. Vet. Med. 113, 34–46. https://doi.org/10.1016/j.prevetmed.2013.10.015

F. Gómez, J. Prieto, J. Galvis, F. Moreno, J. Vargas, 2019. Identification of Super-Spreaders of Foot-and-Mouth Disease in the cattle transportation network: The 2018 outbreak case in Cesar (Colombia), in: 2019 4th World Conference on Complex Systems (WCCS). pp. 1–6.

https://doi.org/10.1109/ICoCS.2019.8930765

Garira, W., 2018. A primer on multiscale modelling of infectious disease systems. Infect. Dis. Model. 3, 176–191. https://doi.org/10.1016/j.idm.2018.09.005

Geale, D.W., Barnett, P.V., Clarke, G.W., Davis, J., Kasari, T.R., 2015. A Review of OIE Country Status Recovery Using Vaccinate-to-Live Versus Vaccinate-to-Die Foot-and-Mouth Disease Response Policies II: Waiting Periods After Emergency Vaccination in FMD Free Countries. Transbound. Emerg. Dis. 62, 388–406. https://doi.org/10.1111/tbed.12165

Goris, N.E., Eblé, P.L., Jong, M.C.M. de, Clercq, K.D., 2009. Quantifying foot-and-mouth disease virus transmission rates using published data. ALTEX - Altern. Anim. Exp. 26, 52–54. https://doi.org/10.14573/altex.2009.1.52

Green, D.M., Kiss, I.Z., Kao, R.R., 2006. Modelling the initial spread of foot-and-mouth disease through animal movements. Proc. R. Soc. B Biol. Sci. 273, 2729–2735. https://doi.org/10.1098/rspb.2006.3648

Grolemund, G., Wickham, H., 2011. Dates and Times Made Easy with {lubridate}. J. Stat. Softw. 40, 1--25.

Guyver-Fletcher, G., Gorsich, E.E., Tildesley, M.J., 2021. A model exploration of carrier and movement transmission as potential explanatory causes for the persistence of foot-and-mouth disease in endemic regions. Transbound. Emerg. Dis. tbed.14423. https://doi.org/10.1111/tbed.14423

Kinsley, A.C., VanderWaal, K., Craft, M.E., Morrison, R.B., Perez, A.M., 2018. Managing complexity: Simplifying assumptions of foot-and-mouth disease models for swine. Transbound. Emerg. Dis. 65, 1307–1317. https://doi.org/10.1111/tbed.12880

Lecoutre, B., 2011. The Bayesian Approach to Experimental Data Analysis, in: Essential Statistical Methods for Medical Statistics. Elsevier, pp. 308–344. https://doi.org/10.1016/B978-0-444-53737-9.50014-1

Machado, G., Farthing, T.S., Andraud, M., Lopes, F.P.N., Lanzas, C., 2021. Modelling the role of mortality-based response triggers on the effectiveness of African swine fever control strategies. Transbound. Emerg. Dis. n/a. https://doi.org/10.1111/tbed.14334

Mahapatra, M., Parida, S., 2018. Foot and mouth disease vaccine strain selection: current approaches and future perspectives. Expert Rev. Vaccines 17, 577–591. https://doi.org/10.1080/14760584.2018.1492378

MAPA, 2022. Plano Estratégico do PNEFA 2017-2026 — Português (Brasil) [WWW Document]. Plano Estratég. PNEFA. URL https://www.gov.br/agricultura/pt-br/assuntos/sanidade-animal-e-vegetal/saude-animal/programas-de-saude-animal/febre-aftosa/plano-estrategico-pnefa-2017-2026 (accessed 5.20.22).

MAPA, 2020. Febre Aftosa [WWW Document]. Minist. Agric. Pecuária E Abast. URL https://www.gov.br/agricultura/pt-br/assuntos/sanidade-animal-e-vegetal/saude-animal/programas-de-saude-animal/febre-aftosa/febre-aftosa (accessed 5.20.22).

Mardones, F., Perez, A., Sanchez, J., Alkhamis, M., Carpenter, T., 2010. Parameterization of the duration of infection stages of serotype O foot-and-mouth disease virus: an analytical review and meta-analysis with application to simulation models. Vet. Res. 41, 45. https://doi.org/10.1051/vetres/2010017

Marino, S., Hogue, I.B., Ray, C.J., Kirschner, D.E., 2008. A methodology for performing global uncertainty and sensitivity analysis in systems biology. J. Theor. Biol. 254, 178–196. https://doi.org/10.1016/j.jtbi.2008.04.011

Marschik, T., Kopacka, I., Stockreiter, S., Schmoll, F., Hiesel, J., Höflechner-Pöltl, A., Käsbohrer, A., Pinior, B., 2021. The Epidemiological and Economic Impact of a Potential Foot-and-Mouth Disease Outbreak in Austria. Front. Vet. Sci. 7.

Mckay, M.D., Beckman, R.J., Conover, W.J., 2000. A Comparison of Three Methods for Selecting Values of Input Variables in the Analysis of Output From a Computer Code. Technometrics 42, 55–61. https://doi.org/10.1080/00401706.2000.10485979

McReynolds, S.W., Sanderson, M.W., Reeves, A., Hill, A.E., 2014. Modeling the impact of vaccination

control strategies on a foot and mouth disease outbreak in the Central United States. Prev. Vet. Med. 117, 487–504. https://doi.org/10.1016/j.prevetmed.2014.10.005

Moreno-Torres, K.I., Delgado, A.H., Branan, M.A., Yadav, S., Stenfeldt, C., Arzt, J., 2022. Parameterization of the durations of phases of foot-and-mouth disease in pigs. Prev. Vet. Med. 202, 105615. https://doi.org/10.1016/j.prevetmed.2022.105615

Muller, K., Wickham, H., A. James, D., Falcon, S., 2021. RSQLite: SQLite Interface for R.

Naranjo, J., Cosivi, O., 2013. Elimination of foot-and-mouth disease in South America: lessons and challenges. Philos. Trans. R. Soc. B Biol. Sci. 368, 20120381. https://doi.org/10.1098/rstb.2012.0381

Noremark, M., Widgren, S., 2014. {EpiContactTrace}: an {R}-package for contact tracing during livestock disease outbreaks and for risk-based surveillance. BMC Vet. Res. 10, 71–71. https://doi.org/10.1186/1746-6148-10-71

PANAFTOSA-OPS/OMS, 2019. Informe de Situación de los Programas de Erradicación de la Fiebre Aftosa en Sudamérica y Panamá, año 2019.

Paton, D.J., Gubbins, S., King, D.P., 2018. Understanding the transmission of foot-and-mouth disease virus at different scales. Curr. Opin. Virol. 28, 85–91. https://doi.org/10.1016/j.coviro.2017.11.013

Pebesma, E., 2018. {Simple Features for R: Standardized Support for Spatial Vector Data}. R J. 10, 439--446. https://doi.org/10.32614/RJ-2018-009

Perez, A.M., Ward, M.P., Carpenter, T.E., 2004. Epidemiological investigations of the 2001 foot-and-mouth disease outbreak in Argentina. Vet. Rec. 154, 777–782. https://doi.org/10.1136/vr.154.25.777

Prado Siqueira, R., 2021. brazilmaps: Brazilian Maps from Different Geographic Levels.

Probert, W.J.M., Jewell, C.P., Werkman, M., Fonnesbeck, C.J., Goto, Y., Runge, M.C., Sekiguchi, S., Shea, K., Keeling, M.J., Ferrari, M.J., Tildesley, M.J., 2018. Real-time decision-making during emergency disease outbreaks. PLOS Comput. Biol. 14, e1006202. https://doi.org/10.1371/journal.pcbi.1006202

R Core Team, 2021. R: A Language and Environment for Statistical Computing. R Foundation for Statistical Computing, Vienna, Austria.

Ringa, N., Bauch, C.T., 2014. Dynamics and control of foot-and-mouth disease in endemic countries: A pair approximation model. J. Theor. Biol. 357, 150–159. https://doi.org/10.1016/j.jtbi.2014.05.010

Roche, S.E., Garner, M.G., Sanson, R.L., Cook, C., Birch, C., Backer, J.A., Dube, C., Patyk, K.A., Stevenson, M.A., Yu, Z.D., Rawdon, T.G., Gauntlett, F., 2015. Evaluating vaccination strategies to control foot-and-mouth disease: a model comparison study. Epidemiol. Infect. 143, 1256–1275. https://doi.org/10.1017/S0950268814001927

Rossi, G., Smith, R.L., Pongolini, S., Bolzoni, L., 2017. Modelling farm-to-farm disease transmission through personnel movements: from visits to contacts, and back. Sci. Rep. 7, 2375. https://doi.org/10.1038/s41598-017-02567-6

Sanson, R., Rawdon, T., Owen, K., Hickey, K., van Andel, M., Yu, Z., 2017. Evaluating the benefits of vaccination when used in combination with stamping-out measures against hypothetical introductions of foot-and-mouth disease into New Zealand: a simulation study. N. Z. Vet. J. 65, 124–133. https://doi.org/10.1080/00480169.2016.1263165

Sanson, R., Yu, Z., Rawdon, T., van Andel, M., 2021. Investigations into a trigger-based approach for initiating emergency vaccination to augment stamping out of foot-and-mouth disease in New Zealand: a simulation study. N. Z. Vet. J. 69, 313–326. https://doi.org/10.1080/00480169.2021.1921069

Sanson, R.L., Dubé, C., Cork, S.C., Frederickson, R., Morley, C., 2014. Simulation modelling of a hypothetical introduction of foot-and-mouth disease into Alberta. Prev. Vet. Med. 114, 151–163. https://doi.org/10.1016/j.prevetmed.2014.03.005

Santos, D.V. dos, Silva, G.S. e, Weber, E.J., Hasenack, H., Groff, F.H.S., Todeschini, B., Borba, M.R.,

Medeiros, A.A.R., Leotti, V.B., Canal, C.W., Corbellini, L.G., 2017. Identification of foot and mouth disease risk areas using a multi-criteria analysis approach. PLOS ONE 12, e0178464. https://doi.org/10.1371/journal.pone.0178464

SEAPI, 2021. Secretaria da Agricultura Pecuaria e Irrigação.

Sellman, S., Tildesley, M.J., Burdett, C.L., Miller, R.S., Hallman, C., Webb, C.T., Wennergren, U., Portacci, K., Lindström, T., 2020. Realistic assumptions about spatial locations and clustering of premises matter for models of foot-and-mouth disease spread in the United States. PLOS Comput. Biol. 16, e1007641. https://doi.org/10.1371/journal.pcbi.1007641

Seymour, R.G., Kypraios, T., O'Neill, P.D., 2022. Bayesian nonparametric inference for heterogeneously mixing infectious disease models. Proc. Natl. Acad. Sci. 119, e2118425119. https://doi.org/10.1073/pnas.2118425119

Shimizu, Y., Hayama, Y., Murato, Y., Sawai, K., Yamaguchi, E., Yamamoto, T., 2020. Epidemiology of Classical Swine Fever in Japan—A Descriptive Analysis of the Outbreaks in 2018–2019. Front. Vet. Sci. 7, 573480. https://doi.org/10.3389/fvets.2020.573480

Singanallur, N.B., Dekker, A., Eblé, P.L., van Hemert-Kluitenberg, F., Weerdmeester, K., Horsington, J.J., Vosloo, W., 2021. Emergency FMD Serotype O Vaccines Protect Cattle against Heterologous Challenge with a Variant Foot-and-Mouth Disease Virus from the O/ME-SA/Ind2001 Lineage. Vaccines 9, 1110. https://doi.org/10.3390/vaccines9101110

Sseguya, I., Mugisha, J.Y.T., Nannyonga, B., 2022. Outbreak and control of Foot and Mouth Disease within and across adjacent districts—A mathematical perspective. Results Control Optim. 6, 100074. https://doi.org/10.1016/j.rico.2021.100074

Stenfeldt, C., Diaz-San Segundo, F., de los Santos, T., Rodriguez, L.L., Arzt, J., 2016. The Pathogenesis of Foot-and-Mouth Disease in Pigs. Front. Vet. Sci. 3.

Teboh-Ewungkem, M.I., Ngwa, G.A. (Eds.), 2021. Infectious Diseases and Our Planet, Mathematics of Planet Earth. Springer International Publishing, Cham. https://doi.org/10.1007/978-3-030-50826-5

Thompson, D., Muriel, P., Russell, D., Osborne, P., Bromley, A., Rowland, M., Creigh-Tyte, S., Brown, C., 2002. Economic costs of the foot and mouth disease outbreak in the United Kingdom in 2001. Rev. Sci. Tech. 21, 675–687.

Tildesley, M.J., Smith, G., Keeling, M.J., 2012. Modeling the spread and control of foot-and-mouth disease in Pennsylvania following its discovery and options for control. Prev. Vet. Med. 104, 224–239. https://doi.org/10.1016/j.prevetmed.2011.11.007

van Andel, M., Tildesley, M.J., Gates, M.C., 2021. Challenges and opportunities for using national animal datasets to support foot-and-mouth disease control. Transbound. Emerg. Dis. 68, 1800–1813. https://doi.org/10.1111/tbed.13858

van Roermund, H.J.W., Eblé, P.L., de Jong, M.C.M., Dekker, A., 2010. No between-pen transmission of foot-and-mouth disease virus in vaccinated pigs. Vaccine 28, 4452–4461. https://doi.org/10.1016/j.vaccine.2010.04.019

Ward, M.P., Highfield, L.D., Vongseng, P., Graeme Garner, M., 2009. Simulation of foot-and-mouth disease spread within an integrated livestock system in Texas, USA. Prev. Vet. Med. 88, 286–297. https://doi.org/10.1016/j.prevetmed.2008.12.006

Wickham, H., Averick, M., Bryan, J., Chang, W., McGowan, L., François, R., Grolemund, G., Hayes, A., Henry, L., Hester, J., Kuhn, M., Pedersen, T., Miller, E., Bache, S., Müller, K., Ooms, J., Robinson, D., Seidel, D., Spinu, V., Takahashi, K., Vaughan, D., Wilke, C., Woo, K., Yutani, H., 2019. Welcome to the Tidyverse. J. Open Source Softw. 4, 1686. https://doi.org/10.21105/joss.01686

Ziegel, E.R., Lohr, S.L., 2000. Sampling: Design and Analysis. Technometrics 42, 223. https://doi.org/10.2307/1271491

Supplementary Material

Modeling foot-and-mouth disease dissemination in Brazil and evaluating the effectiveness of control measures

Nicolas C. Cardenas[1], Francisco P. N. Lopes[2], Gustavo Machado[1,*]

Running title: Foot-and-mouth disease dissemination across species.

[1] Department of Population Health and Pathobiology, College of Veterinary Medicine, North Carolina State University, Raleigh, NC, USA

[2] Departamento de Defesa Agropecuária, Secretaria da Agricultura, Pecuária e Desenvolvimento Rural, Porto Alegre, Brazil
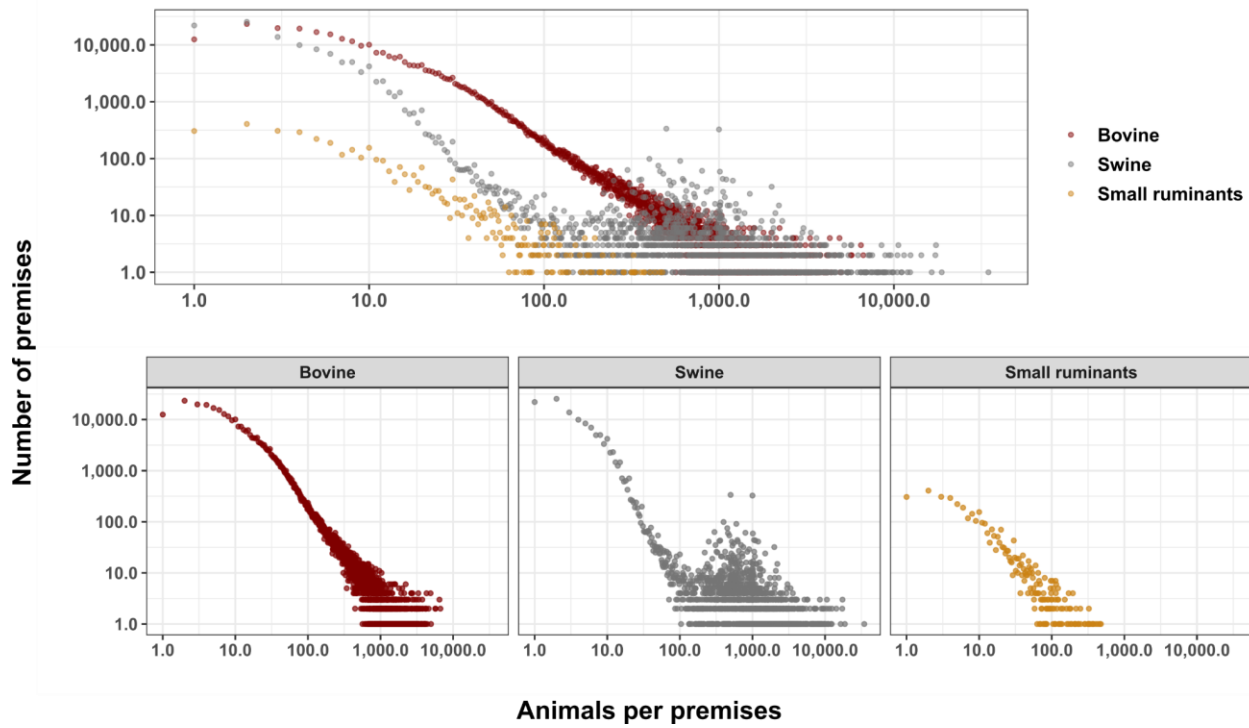
Supplementary Figure S1. The 2018 distribution of farm-level population for each species in the state of Rio Grande do Sul, Brazil. The y-axis is the number of farms and the x-axis is the number of animals, both on a log10 scale.
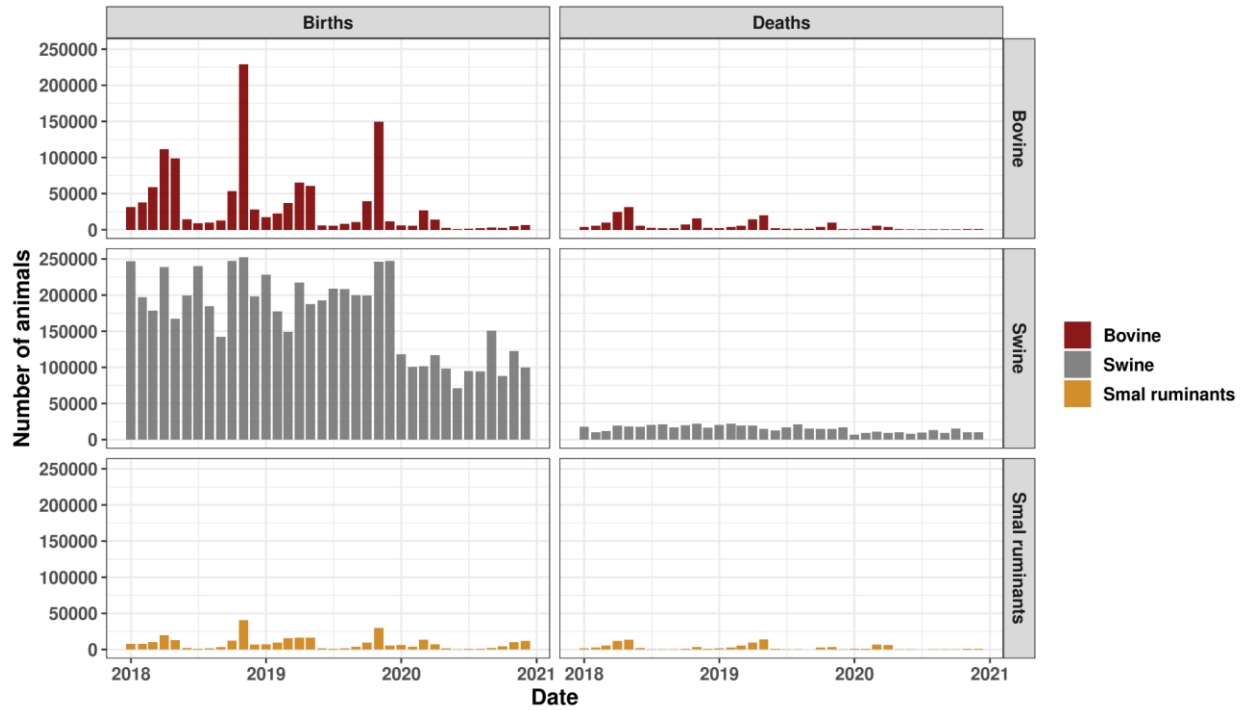
Supplementary Figure S2. The monthly distribution of animal births and deaths by species, from January 1st, 2018 to December 31st, 2020.

bioRxiv preprint doi: https://doi.org/10.1101/2022.06.14.496159; this version posted July 29, 2022. The copyright holder for this preprint (which was not certified by peer review) is the author/funder, who has granted bioRxiv a license to display the preprint in perpetuity. It is made available under aCC-BY-NC-ND 4.0 International license.
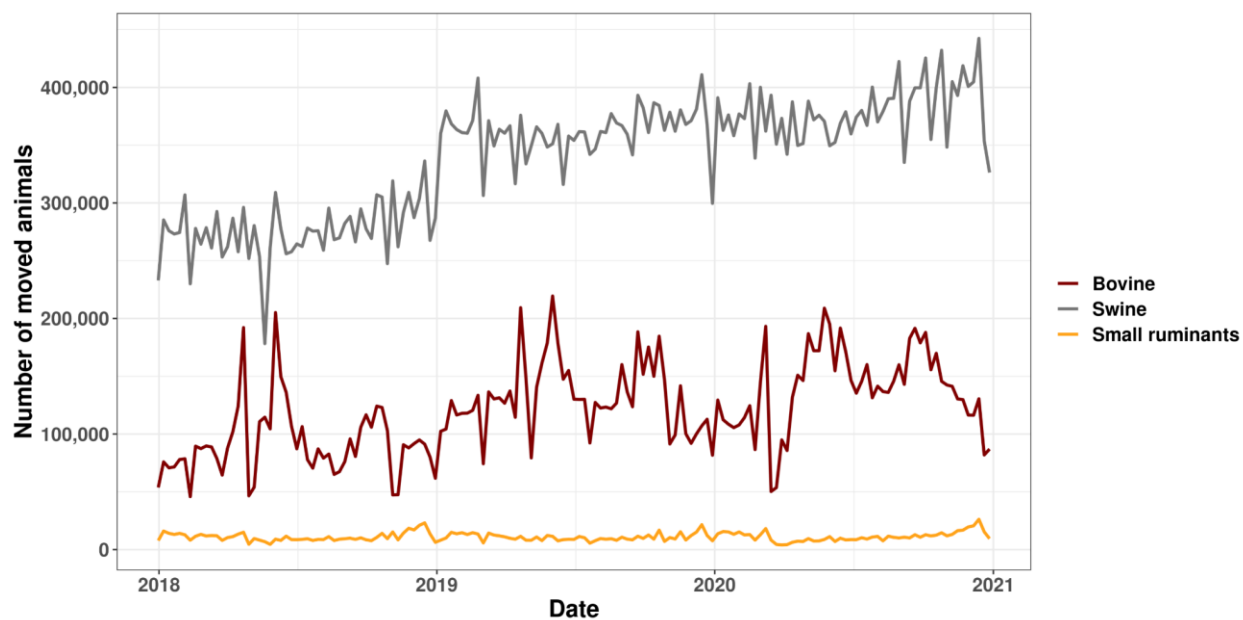
Supplementary Figure S3. The weekly between-farm animal movements, from January 1st,

2018 to December 31st, 2020.
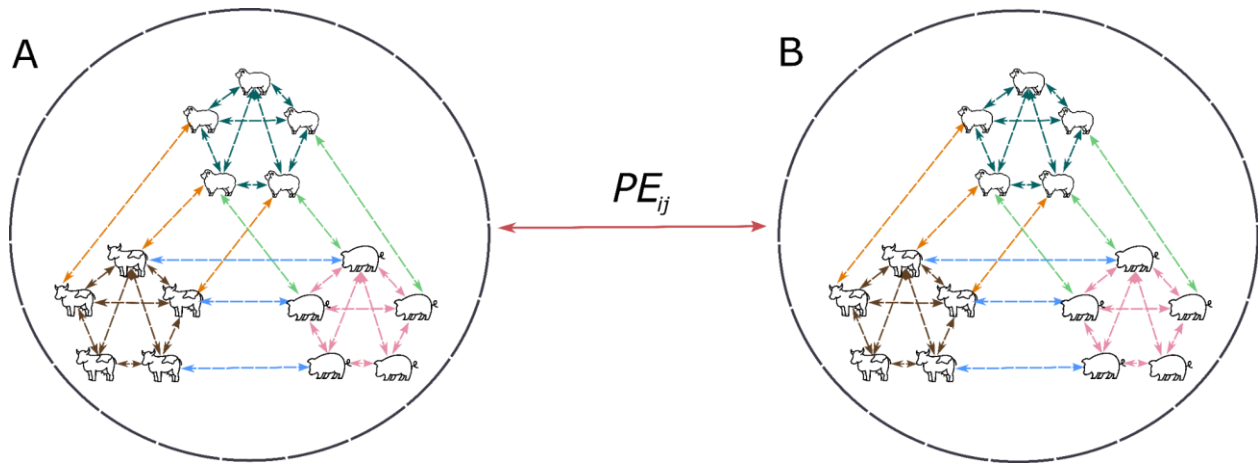
Supplementary Figure S4. Representation of the different population interactions at the within-farm level. For this example, we considered farms with all three species. The dashed line represents the interaction within and between species, and the color denotes a β for each host-to-host interaction (Table 2). The solid line represents the interaction among the farms with different infection probabilities modulated by the spatial proximity (spatial transmission). PE denotes the transmission probability given a distance between farm i to farm j.
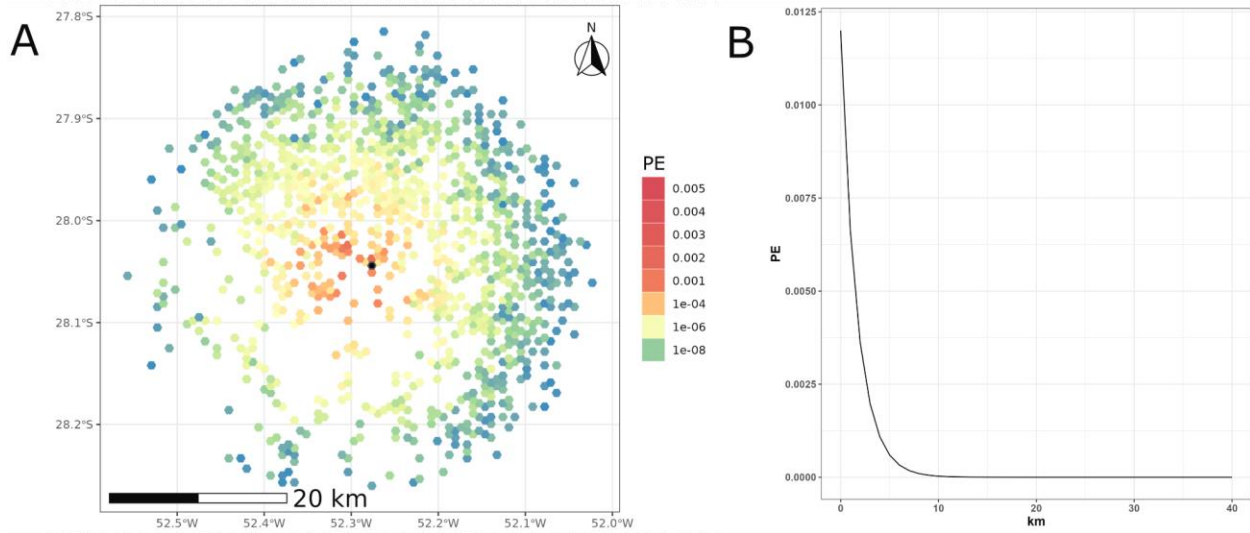
Supplementary Figure S5. A) Representation of grid-hexagons of size 0.76 km (503,516 m^2).

Each hexagon can host one or more farm locations. The color of the hexagon represents the

probability of PE exposure assuming ten infected animals in the center (black hexagon). B) PE

distance in km.
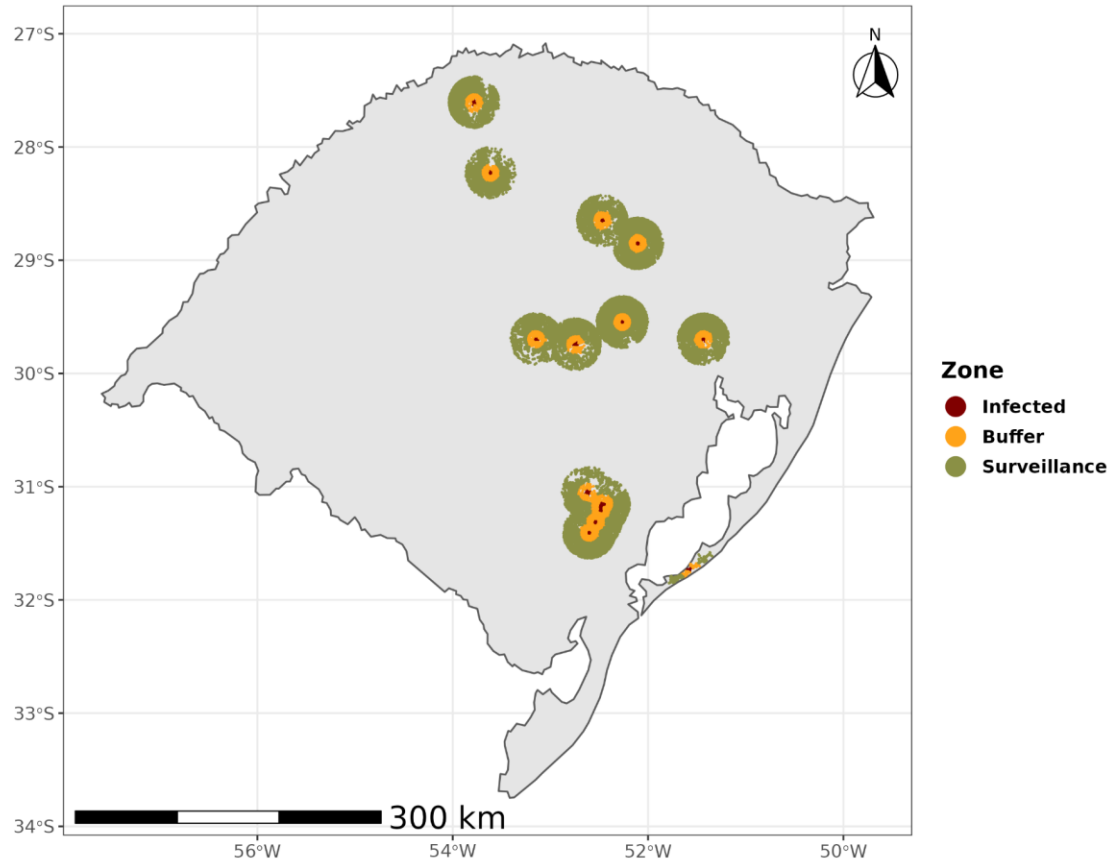
Supplementary Figure S6. **Control zones mapping.** The infected control zones of 3 km are represented as red dots, the 7 km buffer zone is represented as yellow dots, and the 15 km surveillance zone is represented as green dots. Of note, control zones with overlapping are merged.
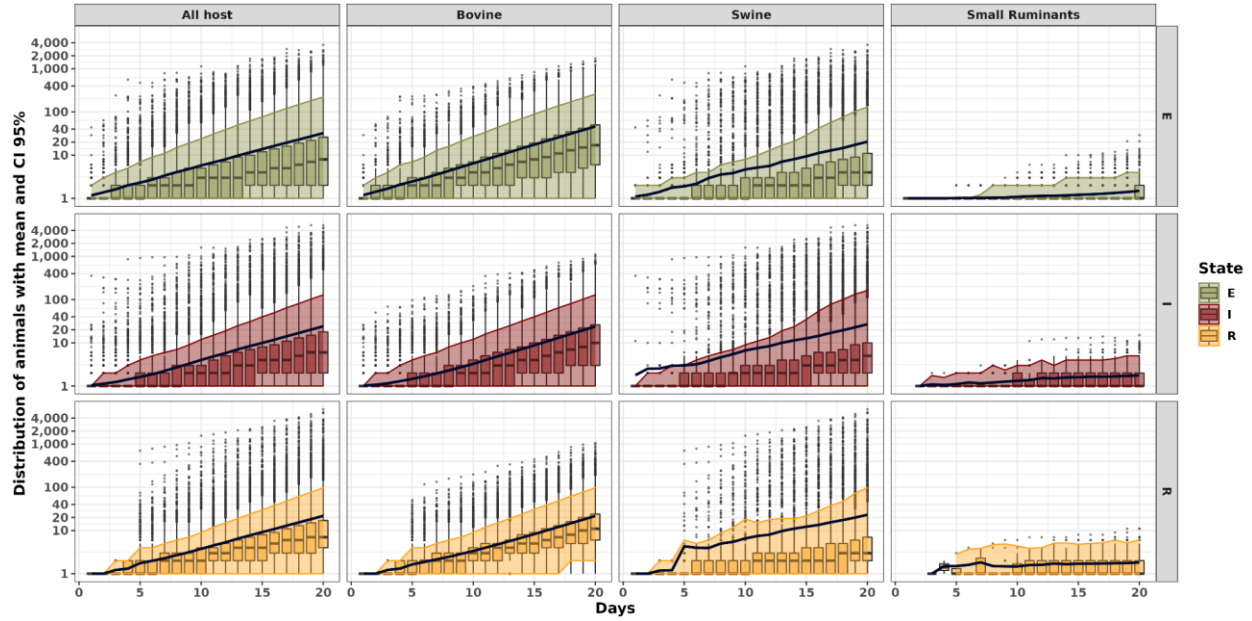
Suplementary Figure S7. Distribution of animals per compartment, exposed (E), infected (I), and recovered (R) by species. Because the number of susceptible animals is very large (19,267,676), the S compartment is not shown. The solid line represents the mean and the dots are outliers. The colored background area represents the 95% credible interval. The y-axis is on a log10 scale.
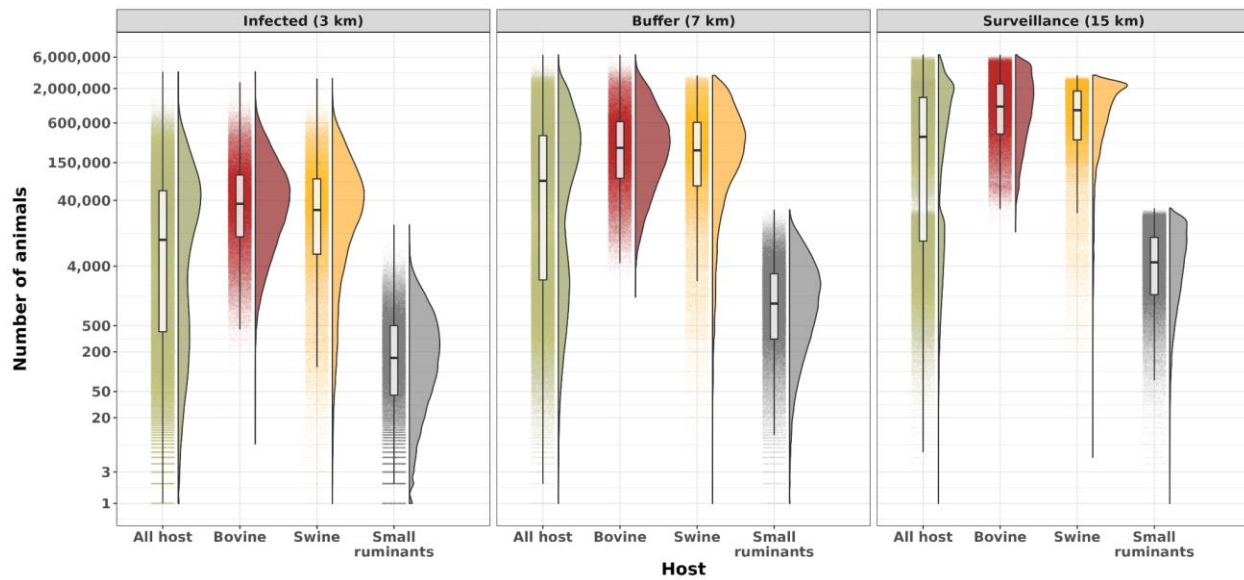
Supplementary Figure S8. The distribution of animals within control zones at 20 days from the initial infection. The y-axis shows the number of animals within infected zones, buffer zones, and surveillance on a log10 scale. The left side boxplots include outliers and the right size density distribution.
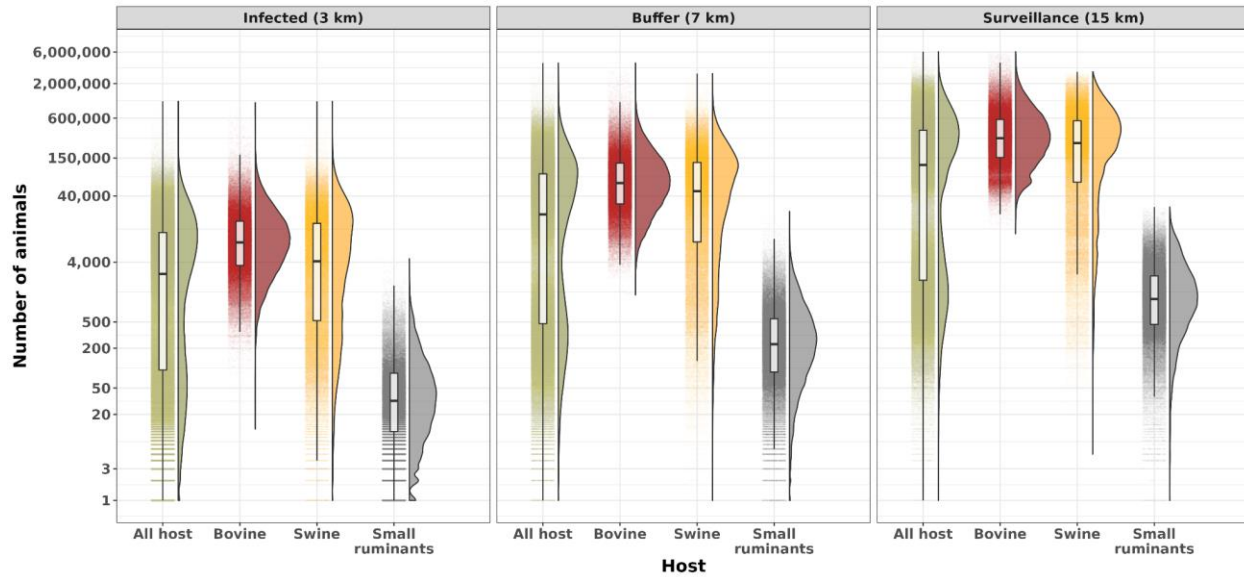
Supplementary Figure S9. The distribution of animals within control zones at 10 days from the initial infection. The y-axis shows the number of animals within infected zones, buffer zones, and surveillance on a log10 scale. The left side boxplots include outliers and the right size density distribution.
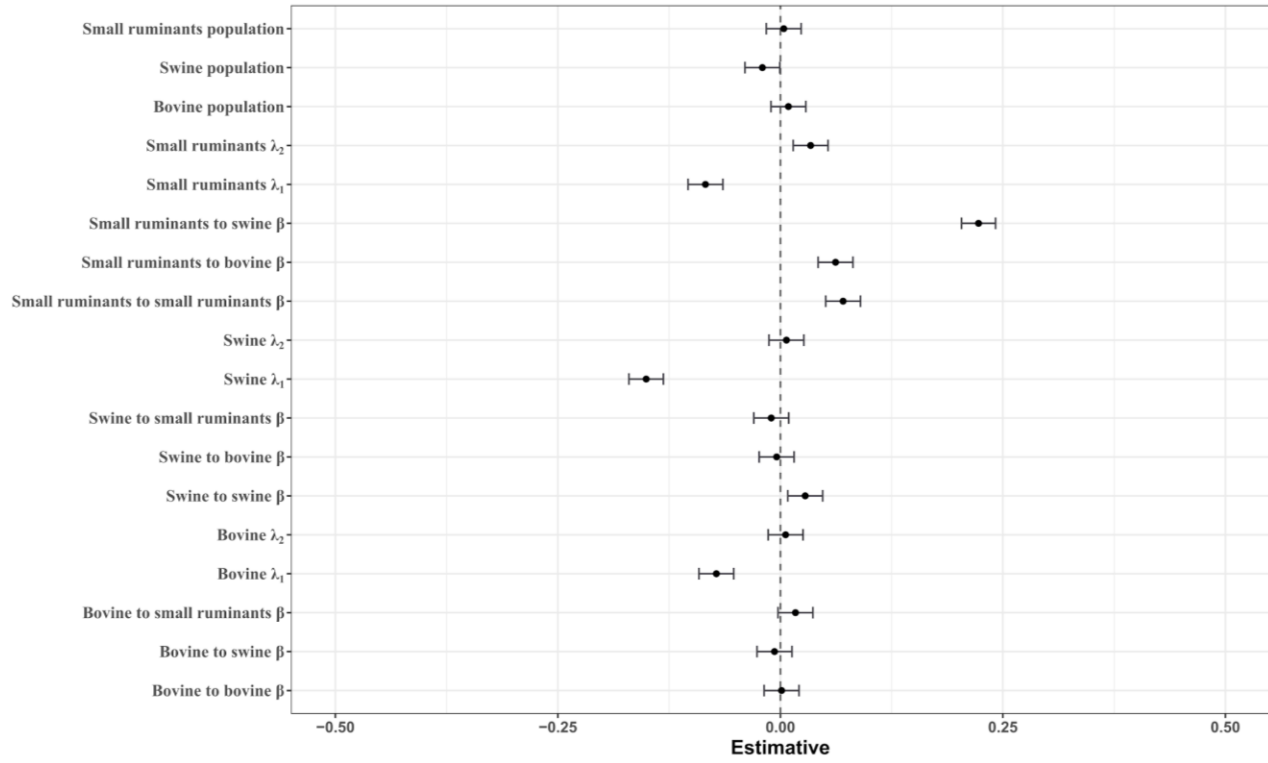
Supplementary Figure S10. Sensitivity of the number of infectious animals to changes over the parameters using LHS-PRCC.

Supplementary Figure S11. The distribution of farms within control zones at 10 days from the initial infection. The y-axis shows the number of animals within infected zones, buffer zones, and surveillance on a log10 scale. The left side boxplots include outliers and the right size density distribution.

Effectiveness of control actions started 10 days after initial simulated infection

At 10 days of FMD dissemination, the baseline control scenario fade out 99.90% of epidemics with a median of 2 (IQR: 1-4, max: 162) infected farms, while scenario one eliminated 99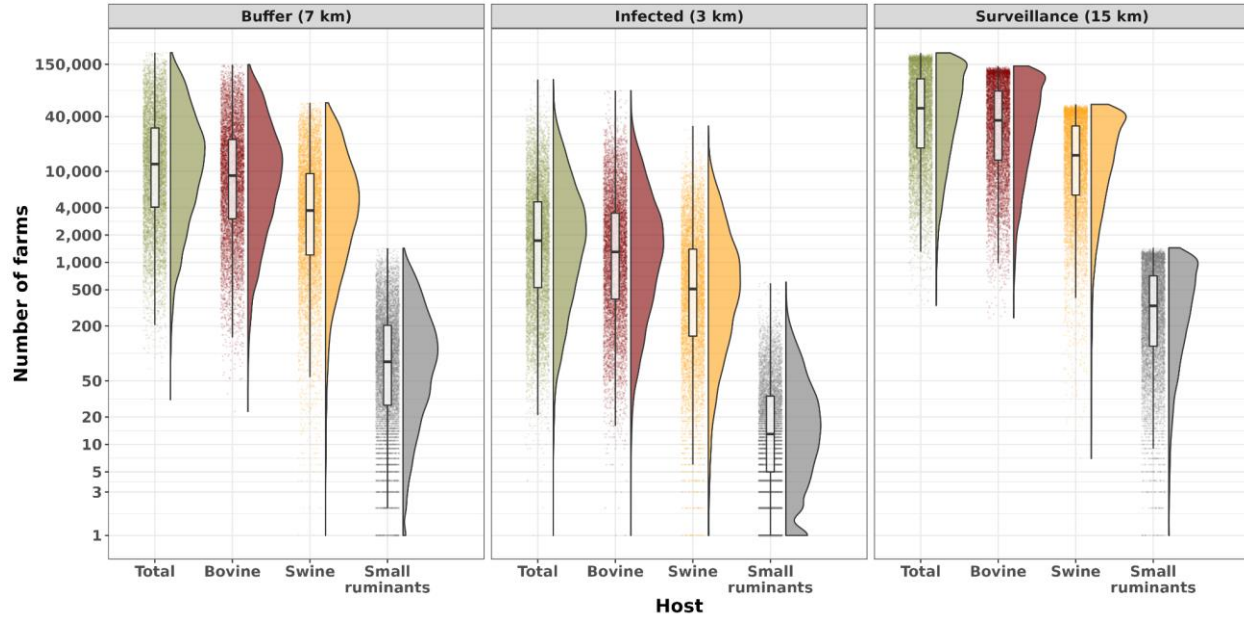.96% of simulated epidemics with a median of 2 (IQR: 1-4, max: 162). Scenario two (depopulation only) eliminated 99.5% of simulated epidemics with a median of 2 (IQR: 1-5, max: 45) infected farms. Scenario three which has three times the depopulation and vaccination of the baseline control scenario was enough to fade out 99.97% of epidemics with a median of 2 (IQR: 1-4, max: 164) initially infected farms (Supplementary Material Figure S12). Similar to the control actions simulations at 20 days scenario two (depopulation only) failed more often and was not able to control epidemics with a median of 30 (IQR: 19-41, max: 248) initially infected farms.

In addition, for simulation that was not able to eliminate simulated epidemics, the baseline control scenario failed in eliminating simulations with a median of 69 (IQR: 40-157, max: 258) infected farms, while scenarios one and three, epidemics with a median of 164 (IQR: 164-202, max: 258) and median of 183 (IQR: 162-216, max: 258), respectively (Supplementary Material Figure S12).
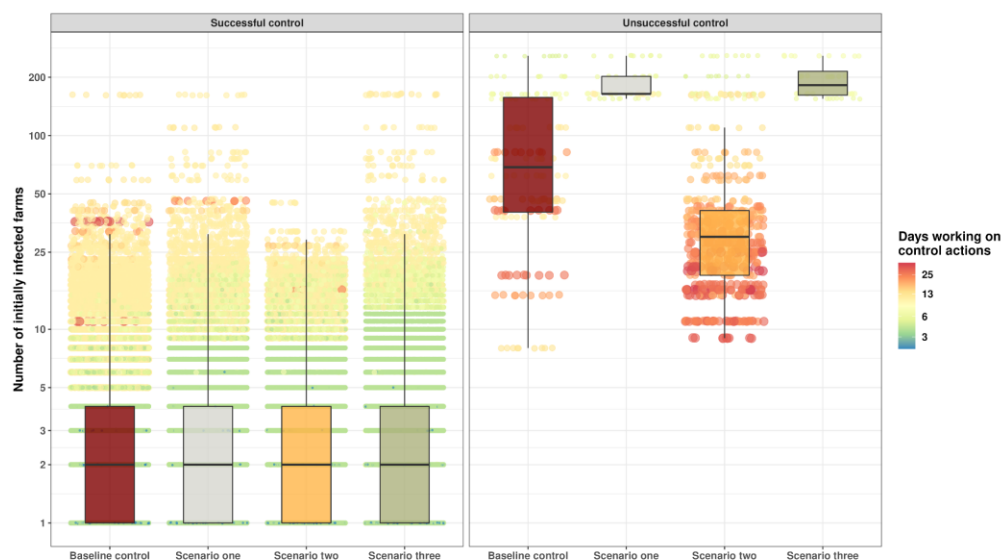
Supplementary Figure S12. The distribution of FMD epidemics successfully and unsuccessfully halted under four control and eradication scenarios after 10 days from the initial seeded infection. The boxplot shows the distribution of secondarily infected farms at 10 days, the background scattered plot shows individual stochastic simulations in which color represents the number of days control and eradication measures were applied.

For the baseline control scenario from the initial deployment of control actions, the maximum average number of infected farms was 51.5, for scenario one 139 farms, 15 farms in scenario two, and 189 in scenario three. Of the successfully halted epidemic, the baseline control scenario took 63 days to fade out epidemics. In comparison with the baseline scenario, scenario two took 53, scenario one 45, and scenario three 28 days (Supplementary Material Figure S13).
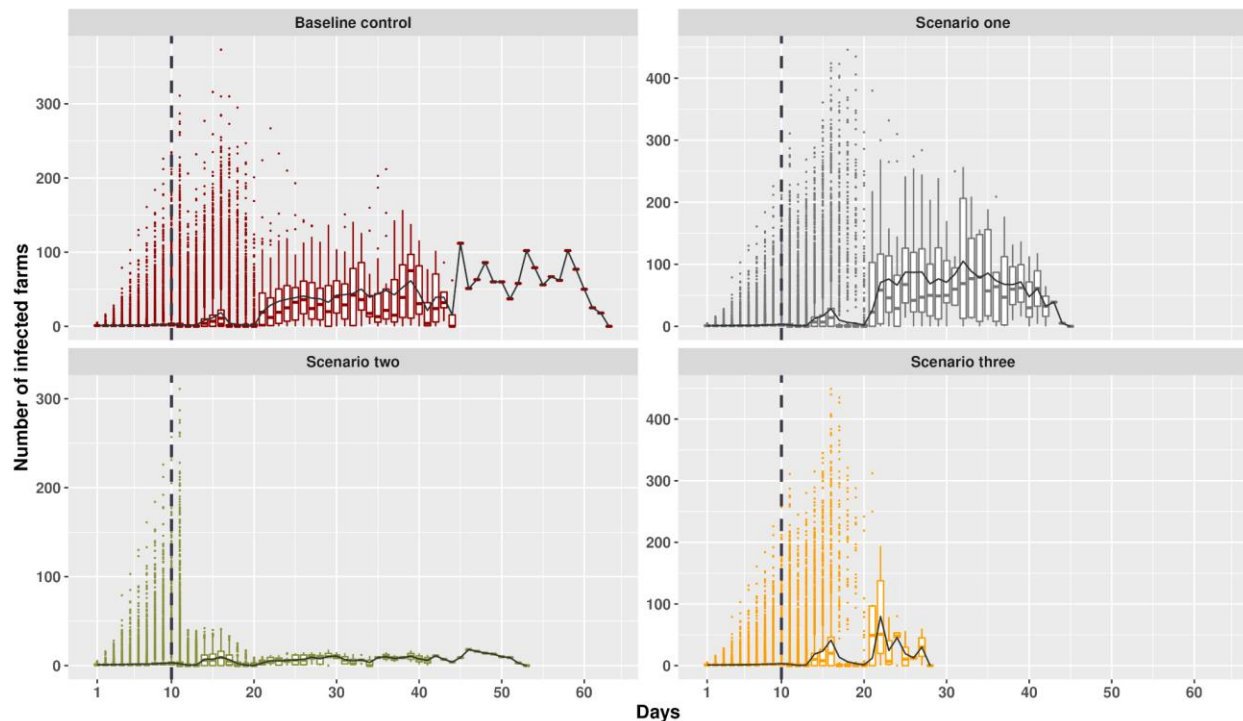
Supplementary Figure S13. The average number of days to stamp out FMD epidemics (of simulation that successfully eliminated outbreaks). The vertical dashed line marks the 10 days of

silent spread and the start of control actions. The solid black line represents the average of infected farms per day. The box plot shows the distribution of secondarily infected farms.
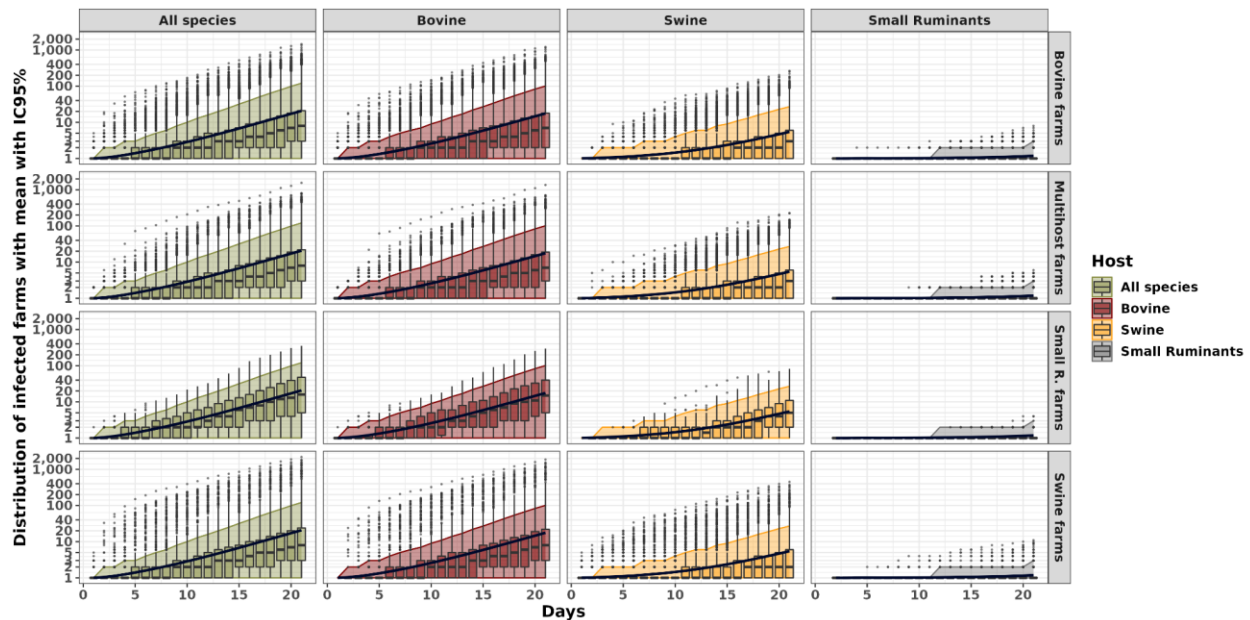
Supplementary Figure S14. Distribution of animals per compartment, exposed (E), infected (I), and recovered (R) by species and by initial farm type where the simulation started. The right y-axis represents the type of farm where the simulation model started. Because the number of susceptible animals is very large (19,267,676), the S compartment is not shown. The solid line represents the mean, and the dots are outliers. The colored background area represents the 95% credible interval. The y-axis is on a log10 scale.
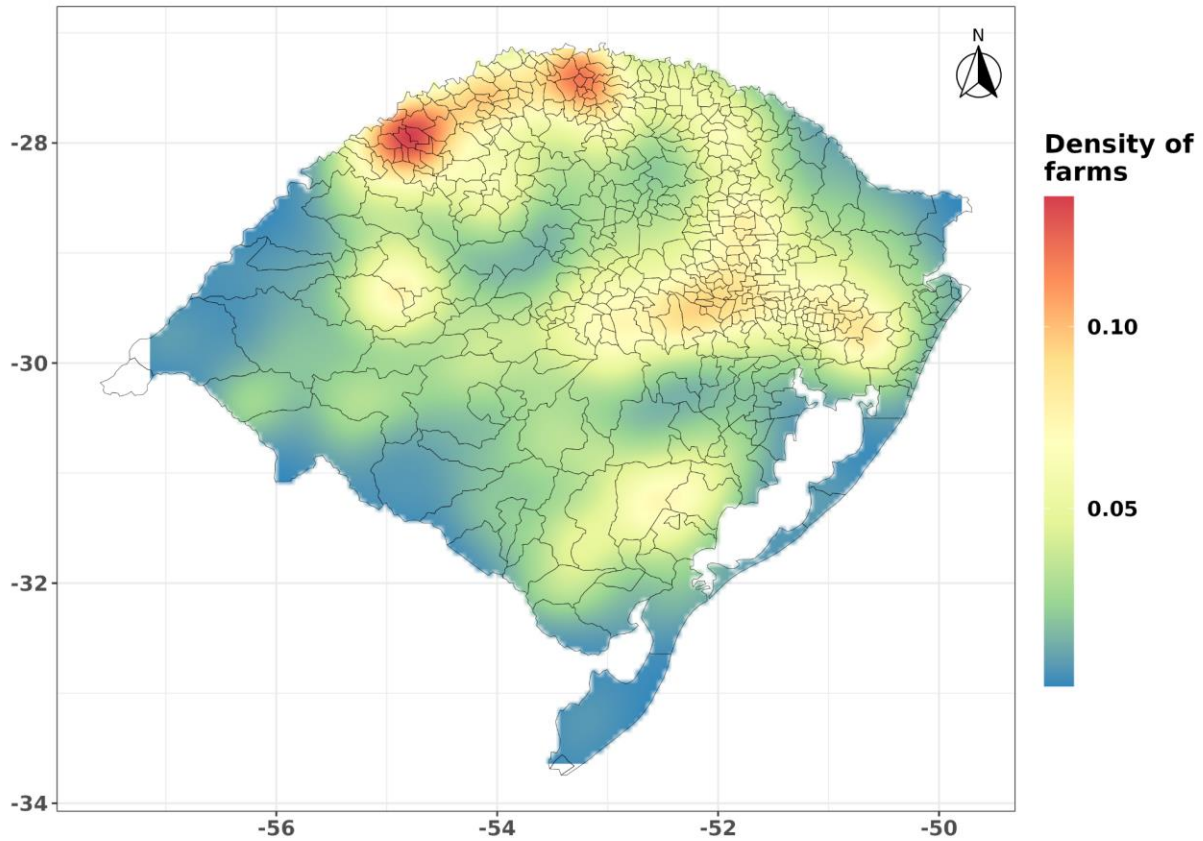
Supplementary Figure S15. Farms density of the Rio Grande do Sul state when considering farms that were not successfully controlled, overall control action simulations across all scenarios. The color background represents the farm density value when considering 0.05 units of the latitude and longitude projection. The solid black line represents the municipalities' boundaries of the state of Rio Grande do Sul.

Supplementary Table S1. Estimated animal-level distribution of at 10 and 20 days after initial infection.

Category	State	Quantile 0.25	Mean	Median	Quantile 0.75	Maximum	Days after initial infection
All species	Susceptible	19,459,735	19,495,401	19,490,270	19,525,934	19,717,989	10
All species	Exposed	2	10	5	10	1,783	10
All species	Infected	1	6	3	6	2,735	10
All species	Recovered	2	5	3	5	2,741	10
Bovine	Susceptible	14,330,643	14,330,468	14,330,608	14,330,506	14,306,163	10
Bovine	Exposed	2	8	4	9	983	10
Bovine	Infected	1	4	2	5	518	10
Bovine	Recovered	2	4	3	5	1,129	10
Swine	Susceptible	4,886,604	4,886,448	4,886,600	4,886,591	4,824,419	10
Swine	Exposed	1	5	2	3	1,318	10

Swine	Infected	1	7	2	3	2,586	10
Swine	Recovered	1	7	2	3	2,579	10
Small ruminants	Susceptible	50,408	50,390	50,403	50,391	49,761	10
Small ruminants	Exposed	1	1	1	2	51	10
Small ruminants	Infected	1	1	1	2	25	10
Small ruminants	Recovered	1	1	1	2	10	10
All species	Susceptible	19,675,945	19,719,056	19,708,463	19,751,901	19,958,581	20
All species	Exposed	8	74	25	72	7,215	20
All species	Infected	5	49	15	41	9,765	20
All species	Recovered	8	39	15	34	12,250	20
Bovine	Susceptible	14,330,578	14,329,352	14,330,292	14,329,318	14,218,361	20
Bovine	Exposed	7	56	21	61	4,149	20
Bovine	Infected	4	29	12	32	2,636	20

Bovine	Recovered	7	27	14	30	2,768	20
Swine	Susceptible	4,886,599	4,885,767	4,886,577	4,886,129	4,740,943	20
Swine	Exposed	2	23	5	14	4,098	20
Swine	Infected	2	28	5	12	8,082	20
Swine	Recovered	2	22	4	7	10,234	20
Small ruminants	Susceptible	50,407	50,384	50,401	50,384	49,669	20
Small ruminants	Exposed	1	2	1	2	154	20
Small ruminants	Infected	1	2	1	2	166	20
Small ruminants	Recovered	1	2	1	2	132	20

Supplementary Table S2. Estimated number of infected farms at 10 and 20 days after initial infection.

Category	Quantile 0.25	Mean	Median	Quantile 0.75	Maximum	Days after initial infection
All species	1	3.37	2	4	470	10
Bovine	1	3.02	2	4	389	10
Swine	1	1.57	1	2	90	10
Small ruminants	1	1.02	1	1	4	10
All species	3	20.75	8	22	2,197	20
Bovine	3	17.62	7	18	1,862	20
Swine	1	5.45	3	6	450	20
Small ruminants	1	1.18	1	1	11	20

Supplementary Table S3. Summary statistics for animal movement and spatial transmission.

We show the distribution of newly infected animals after 10 and 20 days of FMD dissemination

Route of transmission	Species	Quantile 0.25	Mean	Median	Quantile 0.75	Maximum	Days after initial infection
Animal movement	Bovine	1	2.4	1	16	188	10
Animal movement	Swine	1	7.5	1	58.975	1120	10
Animal movement	Small ruminants	1	1.1	1	2	5	10
Animal movement	All species	1	4.9	1	23	1120	10
Spatial transmission	Bovine	1	2.5	1	9	206	10
Spatial transmission	Swine	1	1.4	1	4	38	10
Spatial transmission	Small ruminants	1	1.0	1	1	2	10
Spatial transmission	All species	1	2.7	2	10	245	10
Animal movement	Bovine	1	4.5	1	32	467	20
Animal movement	Swine	1	11.4	1	123	1617	20
Animal movement	Small ruminants	1	1.4	1	3	105	20
Animal movement	All species	1	11.0	1	95.6	1639	20
Spatial transmission	Bovine	1	10.7	5	57	529	20
Spatial transmission	Swine	1	3.1	2	13	90	20

| Spatial transmission | Small ruminants | 1 | 1.1 | 1 | 2 | 4 | 20 |
| Spatial transmission | All species | 1 | 12.1 | 5 | 65 | 617 | 20 |

Supplementary Table S4. Statistics summary of the number of animals in each control zones after 10 and 20 days of FMD dissemination.

Zone	Species	Quantile 0.25	Mean	Median	Quantile 0.75	Maximum	Days after initial infection
Infected	All host	47	8,748.78	1,833	10,078	1,081,512	10
Infected	Bovine	3,560	13,997.84	7,935	16,649	1,031,244	10
Infected	Swine	496	12,184.92	4,028	15,336	1,081,512	10
Infected	Small ruminants	2	63.56	18	62	4,529	10
Buffer	All host	435	66,309.93	20,151	85,476	4,100,452	10
Buffer	Bovine	30,453	103,109.40	62,935	125,653	4,100,452	10
Buffer	Swine	8,047.25	95,344.95	47,321.5	128,585	2,839,570	10
Buffer	Small ruminants	76	475.44	217	541	23,352	10
Surveillance	All host	2,112	278,247.19	117,367	393,387	6,090,216	10
Surveillance	Bovine	152,906	449,516.51	299,849	573,640	6,090,216	10
Surveillance	Swine	6,4614.25	383,209.77	252,319	548,438	3,019,033	10
Surveillance	Small ruminants	452	2,015.28	1,098	2,466	27,256	10

23

Infected	All host	308	53,434.84	8,660	53,783	3,595,388	20
Infected	Bovine	11,169	84,844.08	35,665	97,155	3,595,388	20
Infected	Swine	6,007	7,5074.99	28,463	84,868	2,853,501	20
Infected	Small ruminants	27	385.46	129	450	17,036	20
Buffer	All Species	2,408	320,223.14	77,679	384,439	6,504,836	20
Buffer	Bovine	87,028	501,054.35	250,295	631,415	6,504,836	20
Buffer	Swine	66,341	457,269.51	230,509	611,856	3,162,750	20
Buffer	Small ruminants	297	2,345.56	1,059	3,046	28,802	20
Surveillance	All host	9,599	885,913.31	369,541	1,460,202	6,546,421	20
Surveillance	Bovine	406,570	1,554,385.98	1,065,027	2,337,789	6,546,421	20
Surveillance	Swine	332,548	1,096,357.88	936,872	1,835,041	3,190,801	20
Surveillance	Small ruminants	1,475	6,996.05	4,581	10,959	30,615	20

Supplementary Table S5. Statistics summary of the number of farms in each control zones after 10 and 20 days of spread disease simulation

Area	Specie	Quantile 0.25	Mean	Median	Quantile 0.75	Maximum	Days after initial infection
Infected	Total	529	4,163	1,736	4,632	102,232	10
Infected	Bovine	395	3,129	1,305	3,481	77,273	10
Infected	Swine	152	1,265	507	1,387	31,567	10
Infected	Small ruminants	3	26	11	30	608	10
Buffer	Total	4,058	23,950	12,032	29,995	202,441	10
Buffer	Bovine	3,022	17,869	8,988	22,397	149,288	10
Buffer	Swine	1,206	7,443	3,711	9,462	56,669	10
Buffer	Small ruminants	26	157	79	199	1,431	10
Surveillance	Total	18,034	65,564	49,450	104,070	200,581	10

Surveillance	Bovine	13,334	47,883	36,420	76,477	144,105	10
Surveillance	Swine	5,499	19,232	15,042	31,569	54,601	10
Surveillance	Small ruminants	120	445	332	710	1,447	10
Infected	Total	583	4,222	1,785	4,804	164,089	20
Infected	Bovine	431	3,176	1,333	3,610	123,200	20
Infected	Swine	165	1,282	521	1,454	50,188	20
Infected	Small ruminants	3	27	11	31	1,114	20
Buffer	Total	4,357	24,247	12,303	30,900	216,163	20
Buffer	Bovine	3,240	18,082	9,177	23,106	156,541	20
Buffer	Swine	1,299	7,517	3,791	9,707	59,156	20
Buffer	Small ruminants	28	159	82	204	1,548	20
Surveillance	Total	19,295	66,457	50,148	105,943	203,462	20

Surveillance	Bovine	14,187	48,514	36,858	77,700	147,013	20
Surveillance	Swine	5,817	19,456	15,346	31,937	55,281	20
Surveillance	Small ruminants	128	453	340	720	1,498	20

Supplementary Table S6. Results for the predicted number of epidemics fade out for each control and eradication strategy after 20 days of initial simulated infection.

Scenario	FMD fade out	Number of simulations (%)
Baseline control scenario: Vaccination of 5,000 animals/day + depopulation of 4 farms/day	Successfully control	104,598 (93.39%)
Baseline control scenario: Vaccination of 5,000 animals/day + depopulation of 4 farms/day	Unsuccessfully control	7,407 (6.61%)
Scenario one: Vaccination of 10,000 animals/day) + depopulation of 8 farms/day	Successfully control	109,593 (97.85%)
Scenario one: Vaccination of 10,000 animals/day) + depopulation of 8 farms/day	Unsuccessfully control	2,412 (2.15%)

Scenario two: Depopulation of 8 farms/day	Successfully control	87,759 (78.35%)
Scenario two: Depopulation of 8 farms/day	Unsuccessfully control	24,246 (21.65%)
Scenario three: Vaccination of 15,000 animals/day + depopulation of 12 farms/day)	Successfully control	110,115 (98.31%)
Scenario three: Vaccination of 15,000 animals/day + depopulation of 12 farms/day))	Unsuccessfully control	1,890 (1.69%)